



Living on the slope. The Middle and Upper Paleolithic occupation of Feldberg “Steinacker”

Leben auf dem Hang. Die mittel- und jungpaläolithische Besiedlung von Feldberg „Steinacker“

Marcel BRADTMÖLLER^{1*}, Olaf BUBENZER², Stefan HECHT², Diethard TSCHOCKE³, Aitor CALVO^{4,5}, Arantzazu Jindriska PÉREZ FERNÁNDEZ^{6,7}, Christoph SCHMIDT⁸, Joao MARREIROS^{9,10}, Felix HENSELOWSKY¹¹, Merlin HATTERMANN⁴, Lisa BAUER¹ & Marcel EL-KASSEM¹²

- ¹ Heinrich Schliemann-Institute for Ancient Studies, Universität Rostock, Neuer Markt 3, 18055 Rostock, Germany; email: marcel.bradtmoeller@uni-rostock.de [MB]; lcbauer@posteo.de [LB]
- ² Geographisches Institut, Universität Heidelberg, Im Neuenheimer Feld 348, 69120 Heidelberg, Germany; email: olaf.bubenzler@uni-heidelberg.de [OB]; stefan.hecht@uni-heidelberg.de [SH]
- ³ Landesamt für Denkmalpflege im Regierungspräsidium Stuttgart, Dienstsitz Freiburg, Günterstalstraße 67, 79100 Freiburg i. Br., Germany; email: diethard.tschocke@rps.bwl.de
- ⁴ Institut für Ur- und Frühgeschichte, Friedrich-Alexander-Universität Erlangen-Nürnberg, Kochstraße 4/18, 91054 Erlangen, Germany; email: merlin-janis.hattermann@fau.de
- ⁵ Department of Geography, Prehistory and Archaeology, University of the Basque Country (UPV/EHU), Spain; email: aitor.calvo@ehu.eus
- ⁶ Facultad de Letras. Universidad del País Vasco/Euskal Herriko Unibertsitatea (UPV/EHU), Departamento de Geografía, Prehistoria y Arqueología. Area de Prehistoria. Laboratorio de Paleobotánica Lydia Zapata 1.14A, C/Tomás y Valiente s/n 01006, Vitoria-Gasteiz, Spain; email: arantzazujindriska.perez@ehu.eus
- ⁷ Institut für Naturwissenschaftliche Archäologie (INA), Eberhard-Karls-Universität Tübingen, Rümelinstr. 23, 72070 Tübingen, Germany; email: arantzazujindriska.perez@ehu.eus
- ⁸ Institute of Earth Surface Dynamics, University Lausanne, Quartier UNIL-Mouline, Géopolis, 1015 Lausanne, Switzerland; email: christoph.schmidt@unil.ch
- ⁹ TraCEr, Laboratory for Traceology and Controlled Experiments, MONREPOS*. Archaeological Research Centre, and Museum for Human Behavioural Evolution, Schloss Monrepos, D-56567 Neuwied, Germany; email: joao.marreiros@rgzm.de
- ¹⁰ ICArEHB, Interdisciplinary Center for Archaeology and Evolution of Human Behaviour, FCHS, Universidade do Algarve, Portugal
- ¹¹ Geographisches Institut, Johannes-Gutenberg-Universität Mainz, Johann-Joachim-Becher-Weg 21, 55099 Mainz, Germany; email: felix.henselowsky@uni-mainz.de
- ¹² Landesamt für Denkmalpflege im Regierungspräsidium Stuttgart, Dienstsitz Freiburg, Günterstalstraße 67, 79100 Freiburg i. Br., Germany; email: marcel.elkassem@rps.bwl.de

ABSTRACT - This article is dedicated to the Paleolithic open-air site of Feldberg “Steinacker”, located between the Rhine and the Black Forest near Freiburg/Breisgau in South-West Germany. The site was discovered by W. Mähling in 1969 and is primarily known for the presence of tanged points (Font-Robert type), as well as a possible connection via raw material transport to the cave sites of the Swabian Jura. However, stratigraphic context, site formation processes and site function remained unclear. In 2018, the Heritage Management of Baden-Wuerttemberg and the University of Rostock began the first scientific investigations at the site. It was possible to document a knapping area from the Gravettian, presumably in situ. The excavations also revealed a Middle Paleolithic occupation, making “Steinacker” for the moment the only open-air site in South-West Germany where a stratification of Middle to Upper Paleolithic is present. The investigations were accompanied by additional analyses related to site-formation processes and artefact morphology. Geomagnetic and geoelectric prospection as well as sedimentological drilling revealed a complex paleo-relief that was very different from the current topography. Micromorphology and optically stimulated luminescence dating confirmed that the excavated archaeological stratigraphy was largely intact. Moreover, use-wear analysis showed that pieces with strong indications of frost alterations were possibly used on a regular basis at the site.

ZUSAMMENFASSUNG - Der vorliegende Artikel widmet sich der paläolithischen Freilandstation Feldberg „Steinacker“, die sich zwischen Rheinebene und Schwarzwald nahe Freiburg im Breisgau in Südwestdeutschland befindet. Die Fundstelle wurde von

*corresponding author

W. Mähling im Jahr 1969 entdeckt und ist hauptsächlich für ihre Font-Robert-Spitzen sowie eine mögliche Verbindung zu den Höhlenfundplätzen der Schwäbischen Alb bekannt. Insgesamt wissen wir jedoch nur wenig über die Fundstelle selbst. In den letzten Jahren fanden deshalb im Rahmen eines Projekts des Landesamtes für Denkmalpflege im Regierungspräsidium Stuttgart und der Universität Rostock neue wissenschaftliche Untersuchungen an der Fundstelle statt. Dabei war es möglich, Areale mit Grundformproduktion aus der Zeit des Gravettien zu dokumentieren, die sich vermutlich *in situ* befinden. Außerdem wurde mindestens eine mittelpaläolithische Belegung identifiziert, wodurch Feldberg "Steinacker" aktuell die einzige Freilandfundstelle mit einer Stratigraphie vom Mittel- zum Jungpaläolithikum in Südwestdeutschland ist. Die Kampagnen wurden von zahlreichen Nachbardisziplinen begleitet, um Erkenntnisse auf dem Gebiet der Taphonomie und Silexnutzung zu gewinnen. Mikromorphologische Untersuchungen und Lumineszenz-Datierungen weisen auf eine weitgehend intakte lithostratigraphische Abfolge hin. Die geologischen Bohrungen sowie geophysikalischen Messungen bezeugen zudem ein Paläorelief, das sich deutlich von der heutigen Topografie unterscheidet. Darüber hinaus konnte anhand von Gebrauchsspurenanalysen der - möglicherweise regelhafte - Gebrauch kryoklastisch entstandener Trümmer an der Fundstelle belegt werden.

KEYWORDS - Gravettian, Mousterian, open-air site, site-formation processes, use-wear analysis, ERT Survey, Geomagnetic Survey
 Gravettien, Moustérien, Freilandstation, Fundplatzentstehung, Gebrauchsspurenanalyse, Geoelektrik, Geomagnetik

Introduction

Upper Paleolithic research in Southern Baden: A brief overview

Paleolithic investigation on both sides of the Upper Rhine valley dates back to the 19th century, with the first excavations at the Lower/Middle Magdalenian reindeer hunting camp of Munzingen (Ecker 1875, 1877) and at the loess archive of Achenheim (Schumacher 1897). Last not least, fieldwork at the Middle Pleistocene fossil site of Mauer done by Schoentensack (1908) has to be mentioned.

However, only a few sites in this region were investigated systematically during the 20th century (Albrecht 1979, 1981; Albrecht & Hahn 1991; Gersbach 1969; Guenther 1968; Lais 1929-32; Mieg 1901; Padtberg 1925; Peters 1930; Sainty & Thévenin 1978; Zotz 1928). Research after the early 1970s generally focused on the cave sites of the Ach and Lone Valley in the Swabian Jura (Biel 1998). After the turn of the millennium, excavations of the Paleolithic sites in the southern Upper Rhine region were done again (Kind 2008; Koehler et al. 2019, 2021) with re-analysis of old excavations (Pfeifer 2016; Pasda 2017, 2019a, b). One exception of this pattern was the site under study, Feldberg "Steinacker".

The site of Feldberg "Steinacker" – location and vicinity

The southern part of South-West Germany is characterized by three different types of landscapes, a) the Rhine plain, b) the loess-covered foothills (German: „Vorbergzone“) and c) the sub-alpine mountain range of the Black Forest (Fig. 1). The „Steinacker“ site is located in the foothills near the village Feldberg, approximately 40 km south of Freiburg/Breisgau.

The site under study is situated 370 m a.s.l. on the south-eastern slope of the "Steinacker" (engl. "field

of stones"), one of the first mounds of the foothill zone. Within these foothills, several outcrops of high-quality chert are known, which derive from the Jurassic "Kandern Formation" and were partly shifted during the Eocene (cf. Kaiser 2013). Three varieties can be distinguished. Primary deposits at Istein and Kleinkems, sites with Neolithic mining activities (Kaiser 2013), yield a white and greyish type of Rauracien age. This is called "Jurahornstein Typ Rauracien" (engl. "Jurassic chert Type Rauracien", cf. Çep 2013; Kaiser 2013). A second white and greyish variety also occurs in secondary deposits at Hertingen (cf. Kaiser 2013).

Additionally, a third variety, known as chert of Rauracien age, often appears in secondary deposits generally associated with a loam package with bean ore, whose iron salts lead to discoloration (Holdermann 1996). The designation of this type varies from "Bohnerzjaspis" (Kaiser 2013) to "Blutjaspis" (Moreau 2009) or "Bohnerzhornstein Type Rauracien" (engl. "Bean ore chert Type Rauracien", cf. Çep 2013). We follow the latter in this paper. One of these secondary outcrops is apparently located up the slope to the north, only 100-400 m from the site under study (Fig. 2; Mähling 1971).

From the vicinity, several unpublished spots with surface finds of a Paleolithic age are known. One of these is to up the north-western slope of the "Steinacker" hill, providing a lookout into the Rhine valley, up to the Vosges Mountains (Fig. 2, white dot, see discussion). In addition, from the other side of the Mauchener Valley several artefacts of Upper Paleolithic (UP) and especially Middle Paleolithic (MP) age are known (F. Gröteke & G. Lang, personal communication).

However, the nearest well-documented Mid-Upper and/or Middle Paleolithic occupation to the north-west are Achenheim and Mutzig near Strasbourg (Fig. 1: A). To the east, radiocarbon dating on animal

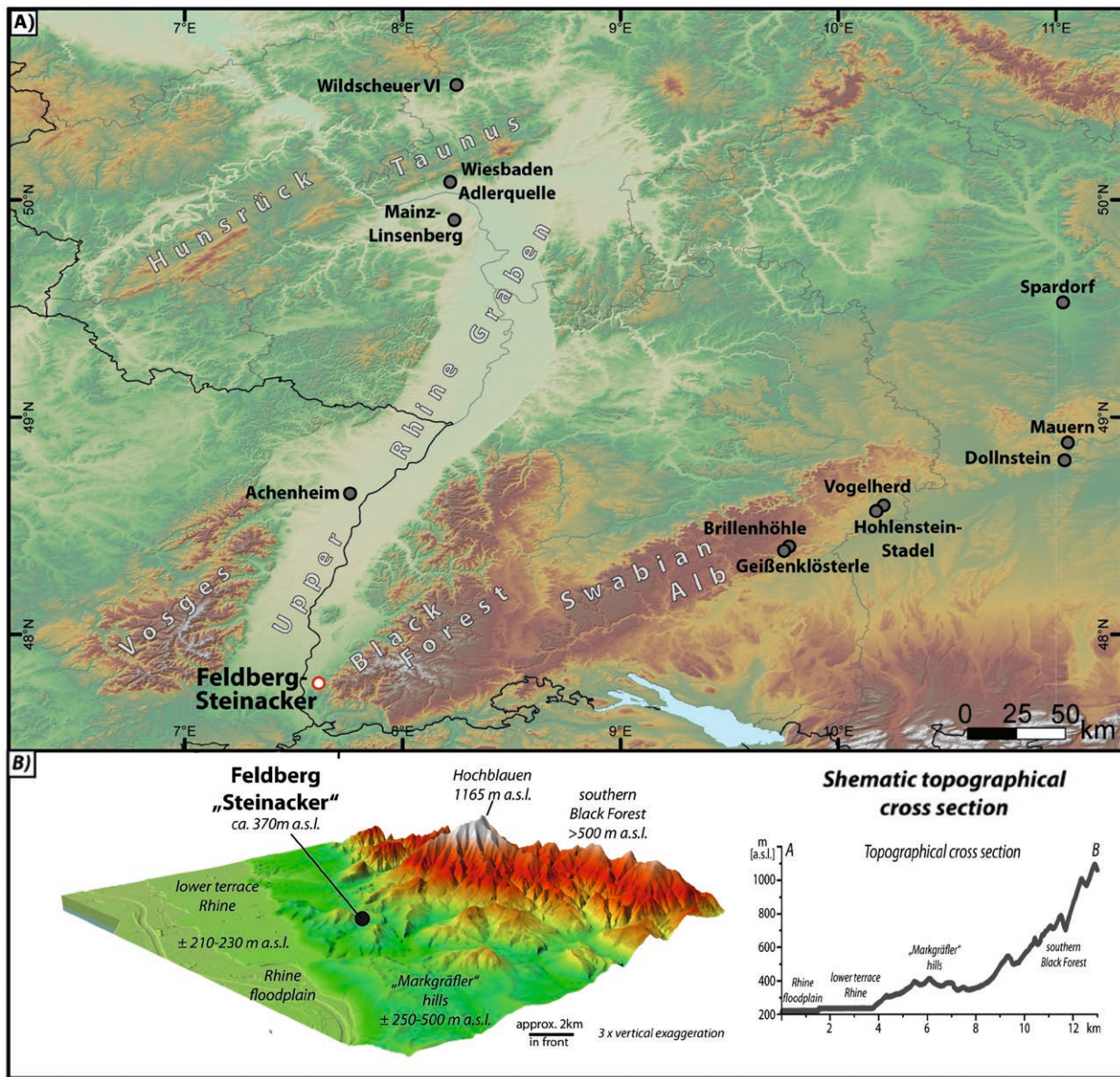


Fig. 1. A: Location of the „Steinacker“ and important Middle- and Upper Paleolithic sites in the vicinity. B: Map with the topographic elements of the surrounding.

Abb. 1. A: Standort des Fundplatzes „Steinacker“ und wichtige mittel- und jungpaläolithische Fundstellen in der weiteren Umgebung. B: Karte mit den topographischen Einheiten im Umfeld des Fundplatzes.

bones with evidence of human modifications suggest presence of Gravettian foragers at Vogelherd and Fetzershaldenhöhle in the Swabian Jura (Barbieri et al. 2021), while lithic assemblages exhibiting low to mid-quantities of "Bohnerzhornstein Type Rauracien" were documented at the sites of Brillenhöhle, Geißenklösterle, Hohle Fels, and Sirgenstein (Moreau 2009). Ultimately, petrological and/or micropaleontological analysis are needed to clarify whether these pieces have been transported across the Black Forest (see Čep 2013).

Research history of the site

While known to local collectors for centuries, the site of Feldberg "Steinacker" was first documented by Werner Emil Adolf Mähling in 1969, an archaeologist

with questionable reputation (Reinhard 2008). Born in 1911 in Berlin, he studied at the Institut für Vor- und Germanische Frühgeschichte in Berlin in the early 1930s. As a member of the paramilitarist arm of the German National Socialist Party (SA since 1933, SS from 1935, Waffen-SS in 1939-40), he took part in the invasion of Denmark and Norway. Afterwards he worked at the „Anstalt für Vor- und Frühgeschichte in Prague" and the „SS Ahnenerbe". After W/W II, he moved to Freiburg/Breisgau and found his way back into archaeology in 1964 as a research assistant at the local Baden-Wuerttemberg State Office for Cultural Heritage Management. During this time, he spotted at "Steinacker" site several large concentrations of Paleolithic stone artefacts while on survey (Mähling 1978). Lacking in-depth knowledge of Paleolithic

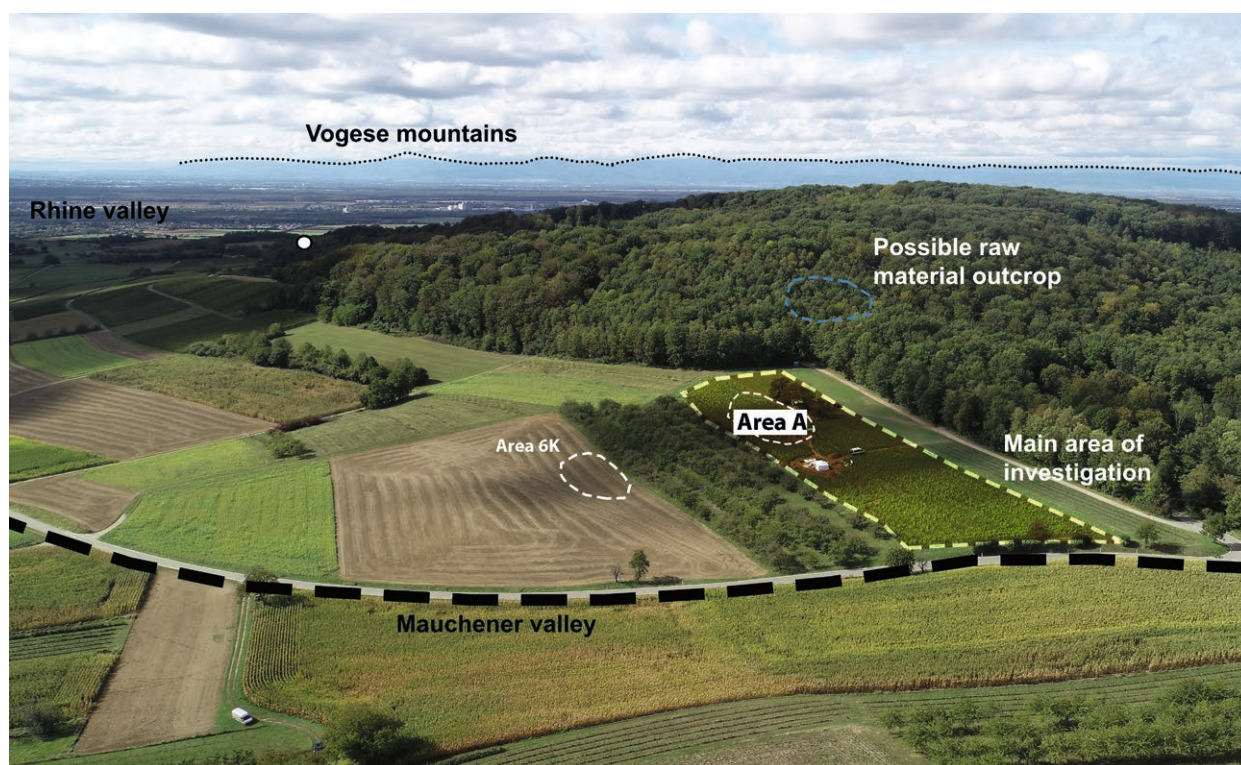


Fig. 2. Aerial Photo of the excavation site (year 2019) with the most important topographic elements. Blue dotted line: Location of an outcrop of the Bohnerzhornstein type Rauracien, after Mähling 1978. White dot: Find spot of a perforated sea urchin.

Abb. 2. Luftbild der Ausgrabungsfläche (Jahr 2019) mit den wichtigsten topographischen Elementen. Blau gestrichelt: Lagerstätte des Bohnerzhornstein Typ Rauracien, n. Mähling 1978. Weißer Punkt: Fundstelle eines perforierten Seeigels.

archaeology, Mähling assumed a Final Paleolithic age for the site, but already classified the tanged point as of possible Gravettian age. However, from 1970 to 1972 Mähling undertook unauthorised excavations on over 100 m² at surface spots with a high artefact density (Holdermann 1996; Mähling 1978).

Due to lack of photographic documentation and an incoherent excavation method (Fig. 3), it has not been possible to locate this excavation, and therefore to integrate this work into the current project. This was also not possible during our geophysical survey, which is maybe related to the fact that we have looked at the



Fig. 3. The only documented profile photos at hand from the Mähling excavation. A: An approximately one meter deep pit of irregular shape. B: Documentation of profile and planum with artefacts after the removal of the plough horizon.

Abb. 3. Die einzig vorliegenden Profilfotos der Ausgrabung Mähling. A: Ein ungefähr ein Meter tiefer Grabungsschnitt mit unregelmäßigen Abmaßen. B: Dokumentation eines Profils und Planums (mit Artefakten) nach dem Abtrag des Pflughorizonts.

wrong place or that the old pits are inconspicuous in the scan due to a heterogeneous backfill.

The lithic assemblages from the excavation (N = 7,540) were later analysed by Holdermann (1996) in an unpublished Master thesis, as well as the surface material by Pasda (1998b). Both supported the Gravettian age model, which was introduced by Ciesla (1992) who clearly identified Font-Robert points within the assemblage. Later, Luc Moreau investigated the assemblage to identify a shaft smoother of sandstone (Moreau et al. 2014).

In 2003, amateur archaeologists from the "prehistory work group" of the Markgräfler Museum Müllheim continued with field surveys, resulting in hundreds of artefacts, which were occasionally published by Braun (2008, 2015, 2021). Among them are well-known tool types from the Upper Paleolithic, such as dihedral burins, micro-gravettes, gravette points and Font-Robert points. Several artefacts also suggested already a Middle Paleolithic beside an Upper Paleolithic occupation.

In 2018, the project presented here was started by the Baden-Wuerttemberg State Office for Cultural Heritage Management and the University of Rostock to re-evaluate the Feldberg "Steinacker" site.

Erosion and ongoing agricultural activities pose a threat to the preservation of the archaeological stratigraphy that might have originally formed at the site. It was therefore necessary to evaluate the situation to see whether undisturbed layers and features are preserved.

Material and Methods

Geophysical survey

Geophysical prospections were carried out in 2018 and 2020 in order to gain insights into the general sub-surface structure and depth of potentially different stratigraphic layers. A geomagnetic survey was conducted 2018 on the agricultural fields containing Areas A and 6K with a manual, five-sensor Sensys magnetometer and a Stonex DGPS receiver system for localisation. Main aim for this survey was to locate the old excavation area and to get a general idea about what kind of archaeological and modern features to expect on the field.

Electrical resistivity tomography (ERT) was used in 2020 to analyse the basic sub-surface characteristics. One ERT-profile (Fig. 4: ERT Steinacker 1) with a length of 75 m was measured using a GeoTOM MK1E100 with Schlumberger configuration, an electrode spacing of 0.75 m with a total of 100 electrodes. The Schlumberger configuration was chosen after tests with different cable configurations as best to distinguish between different loose sediment types. In addition, this configuration has the highest spatial resolution in combination with a low residual error (cp. Hecht et al. 2022). Data processing and electrical resistivity modelling were undertaken using the Res2Dinv

software. Manual drilling was carried out using Pürckhauer and Edelmann to validate the measured features along the profiles. This only addressed the general stratigraphic features of the drill holes in the field and mapped boundaries for interpretation of the geophysical prospection.

The excavations

Four annual campaigns, each of four weeks duration, have so far been conducted, and this paper focuses on the results from 2018, 2019 and 2020. This is mainly due to a delay in laboratory work during Covid-19 restrictions. The starting point of investigation were two areas of high artefact density on the north-eastern slope of the "Steinacker", documented by G. Lang and W. Gröteke in 2003: one in the uppermost field on the slope (Figs. 2 & 4: Area A) and a second, less dense, to the south-west (Figs. 2 & 4: Area 6K).

All excavations so far have been conducted within the framework of a field school with students from Rostock University and staff members of the Baden-Wuerttemberg State Office for Cultural Heritage Management. Apart from the caterpillar trenches (BS 1-4), all trenches were excavated in artificial layers of 5-10 cm depth, with a further subdivision in natural levels when reasonable. All artefacts were measured three-dimensionally using Leica TS total stations within the ETRS/UTM32 reference system (EPSG 25832). The inclination and orientation of all artefacts >1 cm was documented with two coordinates measuring their limitations from 2019 onwards. The backfill was completely water-sieved with a 0.1 cm mesh width. In doing so, the slope was divided into Zone A, encompassing surface concentration A (Fig. 4: Area A), Trench 1 and the north-west part of the Caterpillar Trench BS1 and Zone B, with Trenches BS4, 2, 6, 8 and 9 (Fig. 5).

The first actions undertaken in 2018 were a standardized surface survey and a geomagnetic survey at Area A and Area 6K (Figs. 4 & 6). The main aim of the latter was to identify potential prehistoric features and locating the 1970s excavation area. To document the local stratigraphy, four trenches (1x2 m) were excavated. Trench 1 was set within Area A, and Trenches 2 and 3 were located outside it, within an area with a low find number. In doing so, Pleistocene layers could be documented in Trenches 1-3 in an upper position. In contrast, Trench 4 has shown a completely different setting, with a Holocene colluvium of at least 3 meters in depth.

Due to this situation, the archaeological campaigns of 2019 and 2020 focused on Area A, the backbone of the study at hand. Most of the additional trenches in these two years (Fig. 4: Trenches 6, 8, 9) were excavated close to Trench 2. Trenches 5 and 7, both only 1 m² in size, were used to analyse the uppermost part of the field (Fig. 4). Both were archaeologically sterile. Four trenches of 33 m length in total were also excavated using a Caterpillar in 2019 (Fig. 4: Trench BS 1-4). This

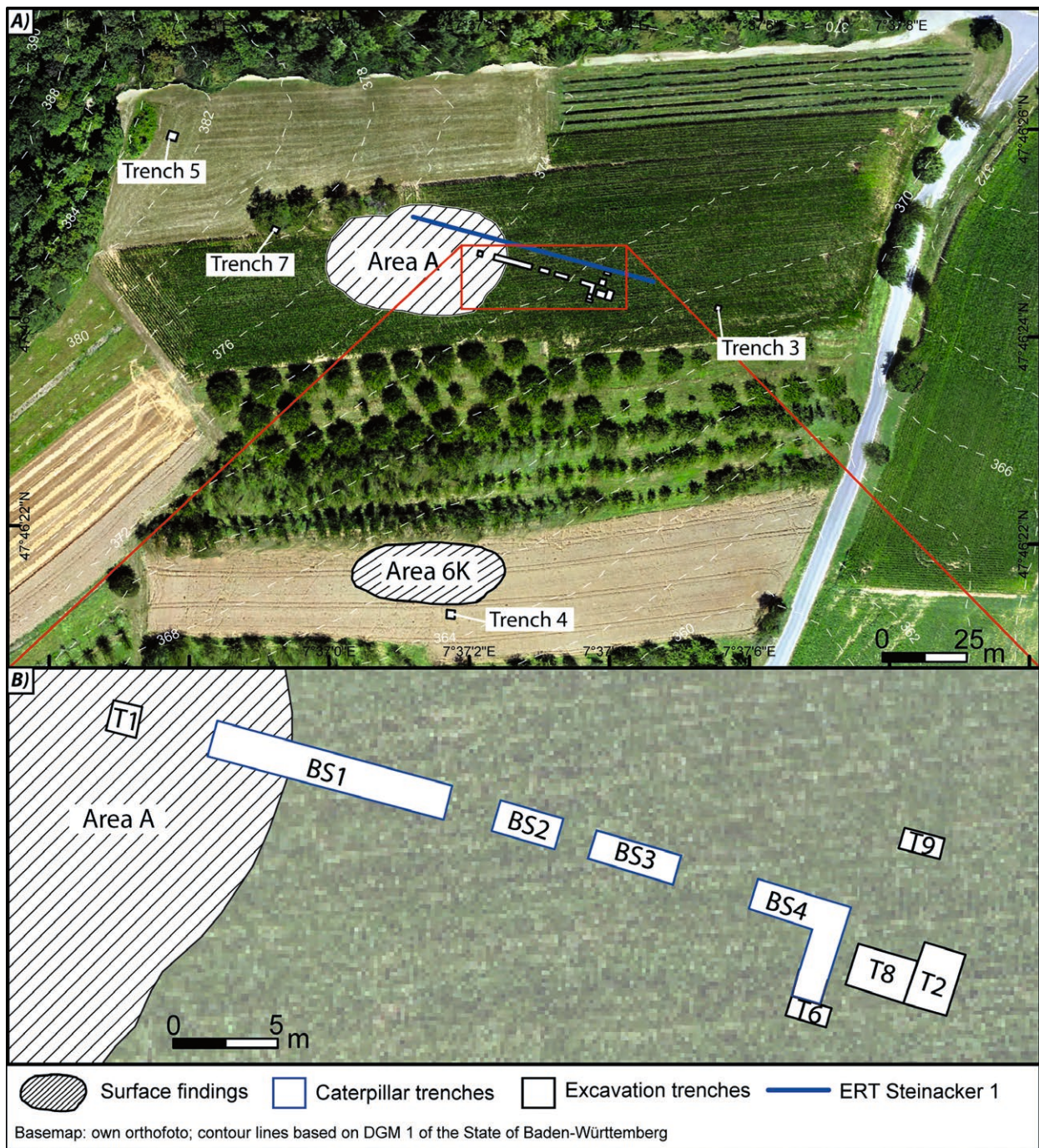


Fig. 4. Excavation plan with the surface concentrations Area A and 6K, the excavation trenches, ERT "Steinacker 1" and drilling locations. Please note that the plan includes the 2021 excavation pits, which are not included into the publication. Oriented to north.

Abb. 4. Plan mit den Oberflächenkonzentrationen A und 6K, den Ausgrabungsschnitten, der ERT Messung „Steinacker 1“ und den Bohrlokalitäten. Bitte beachten, dass hier auch schon die Schnitte der Ausgrabung 2021 eingetragen sind. Nach Norden orientiert.

clearly caused a loss of archaeological material, but the geological profiles became important for understanding of site formation and local paleo-relief.

Lithic assemblages - analysis & use-wear analysis

The artefacts included in this study were discovered during the archaeological excavations in 2018, 2019 and 2020. Some surface finds were used as a comparison.

The excavated assemblage comprises 2,045 lithic finds in total from 12 trenches (Tab. 1). This study

will focus on trenches within and adjacent to Area A (N = 1,991) (Fig. 4: B). Finds from other test trenches (N = 54) will not be included, as well as finds from wet sieving, as they are still under investigation. They will be included within a subsequent publication dedicated specifically to the lithic assemblage.

Lithic analysis mainly followed the type and attribute list given by Drafeh et al. (2008). Additional categories were included to match the special requirements of the assemblage in question. These additions

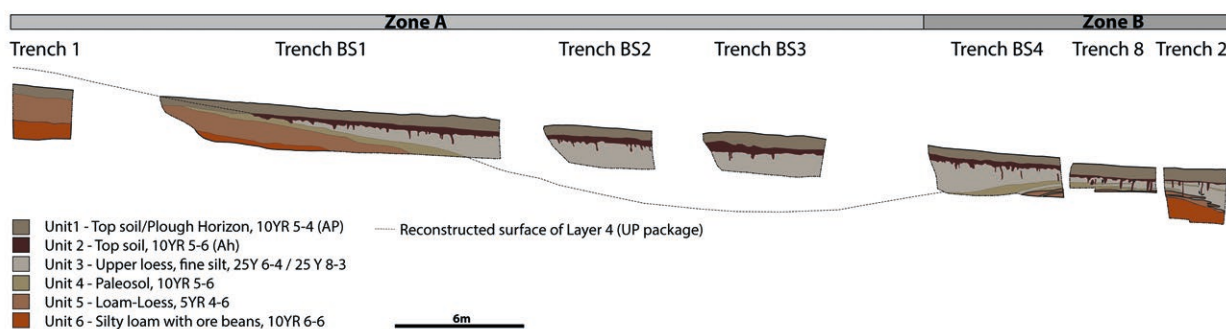


Fig. 5. Cross section of all relevant north profiles.

Abb. 5. Zusammenfassung der relevanten Nordprofile.

mainly involve the use-wear analysis that accompanied the typological and technological considerations. Each find was individually evaluated and incorporated into an Excel database. In doing so, it is important to note that different editors contributed to the lithic analysis. We also started to include unpublished finds from the surface collections of different local amateur archaeologists to gain a general overview about the typological/technological spectrum. These finds are only considered in the discussion.

The two main categories of information are typology/technology and the spatial dataset. As the overall number of finds is quite low, this paper does not aim for a comprehensive lithic analysis on a statistical basis. Furthermore, our analysis is primarily aimed at the most essential trenches (1, 2, 8 and 9).

Use-wear analysis was made on 147 objects. It was mainly focused on assessing the preservation of the lithic surfaces and edges, and in a second step on identifying and describing observed macro and micro traces of use. The macro analysis (fatigue and damage features) was carried out using a 3D digital automated microscope ZEISS Smartzoom 5 (equipped with a PlanApo 1.6x/0.1 objective and an integrated

segmented LED ringlight). The micro-observations of abrasion features were done using a ZEISS Axioscope upright light microscope (EC Epiplan 10x and 20x optical objective). This part of the analysis dealt with finds from Trench 1, 2 and 6.

Micromorphology

A total of 45 sediment samples (dimension of 10x10 cm) were extracted in 2019 from Trench 1 and the Caterpillar trenches (Fig. 4: BS 1-4). Ten of these samples were selected to make thin sections, and further samples of loose sediment were used to run the analyses following established protocols (Courty et al. 1989; Golberg & Macphail 2006). As far as possible at this point, the samples encompassed the entire stratigraphic sequence. The compact sediment samples extracted from the archaeological profile were carefully referenced and covered (Nicosia & Stoops 2017) for the production of thin sections measuring 9x6x30 µm at a commercial lab (Terrascope Thin Section Slides, Troyes, France).

The micromorphological description is elaborated from ten thin sections observed under the microscope (Leica DFC550, Leica DMRX, Zeiss Stemi 2000-C Axio

Archaeological activities		Unmodified blanks		Thermal chunks		Cores		Tools		Other		Total
		N	%	N	%	N	%	N	%	N	%	N
Holdermann 1996	Komplex A	4,787	93.0	na	na	252	4.9	106	2.1	na	na	5,145
	Komplex B	411	90.9	na	na	27	6.0	14	3.1	na	na	452
	Komplex C	1,197	92.4	na	na	59	4.6	39	3.0	na	na	1,295
	Komplex D	606	93.4	na	na	35	5.4	8	1.2	na	na	649
	Total	7,001	92.8	na	na	373	4.9	167	2.2	na	na	7,541
Pasda 1998	Surface 1970 's	na	na	na	na	107	2.2	57	1.1	na	na	5,120
Excavation 2018-2020	Zone A	278	25.2	740	67.0	0	0.0	5	0.5	81	7.3	1,104
	Zone B	259	29.2	413	46.6	2	0.2	9	1.0	204	23.0	887
	Other trenches	14	25.9	31	57.4	0	0.0	0	0.0	9	16.7	54
	Total	537	26.3	1153	56.4	2	0.1	14	0.7	285	13.9	2,045

Tab. 1. Comparison between the newly excavated lithic material (2018-2020) and the assemblages from Mählings actions (surface survey and excavation).

Tab. 1. Vergleich der neu dokumentierten lithischen Funde (2018-2020) mit den Inventaren aus den Aktivitäten Mählings.

Cam MRC with the camera programme of Axio Vision LE64. Rel.4.8 and Zeiss Axio Imager 2) in magnifications between 10x and 400x, with the application of plane polarising light (PPL), crossed (XPL), reflected white light and reflected light fluorescence microscopy. The international standards were followed in describing the microstructure, basal mass, mineral and organic composition and pedofeatures (Bullock et al. 1985; Courty et al. 1989; Fitzpatrick 1984; Stoops 2003).

Luminescence dating

Sample preparation

Twenty-one luminescence samples were taken in steel tubes from cleaned profiles in Trenches 1, 2 and 8 during the 2018, 2019 and 2020 excavations. Since the sediments hosting the archaeological finds at the site are dominated by silt-sized material, luminescence measurements were made on the quartz and polymineral "fine grain" fraction (~4-11 µm). Sample preparation was done in subdued red-light conditions (640 ± 20 nm), and included wet sieving (<63 µm), followed by etching in 10 % HCl and 10 % H₂O₂ to dissolve carbonates and oxidise organic matter, respectively. Settling the grains in a water column for distinct periods (application of Stokes' law) isolated the target grain size of ~4-11 µm. One part of the resulting material was analysed once these steps were completed (the polymineral fine grain fraction), and the other part underwent additional etching in 34 % H₂SiF₆ for at least 7 d, followed by an overnight etch in 10 % HCl to dissolve potential fluorides that might have precipitated (Berger et al. 1980).

Feldspar contamination of the quartz fraction was detected using IR stimulation for all samples, even after prolonged H₂SiF₆ etching (<14 d). The polymineral fraction was therefore used by default for dating, and a dating attempt using a 'double-SAR' approach was made only for two quartz samples (BT1685, BT1686), which showed comparatively low IRSL signal levels (details in the supplementary materials).

Experimental setup, measurement parameters and data reduction

Fine grains were pipetted onto aluminium discs (~2 mg per aliquot) for OSL and IRSL measurements, which were carried out with a Risø TL/OSL DA15 reader equipped with blue (470 ± 5 nm) and infrared (875 ± 80 nm) diodes for signal stimulation, and an EMI 9235QB15 photomultiplier tube coupled with a 7.5 mm Hoya U340 glass filter (quartz) or a Chroma D410/30x interference filter for signal discrimination and detection. Artificial irradiation was carried out with a built-in ⁹⁰Sr/⁹⁰Y β-source delivering a dose rate to fine grains of ~0.120 ± 0.005 Gy s⁻¹.

The single-aliquot regeneration (SAR) protocol (Wintle & Murray 2000) was applied to determine the equivalent dose (D_e) of all samples. Detailed measurement parameters are summarised in the

supplementary materials. As the quartz fraction yielded a non-negligible IRSL signal resulting in IR depletion ratios (Duller 2003) deviating ~10-20 % from unity for most aliquots, we used the 'double-SAR' protocol (Banerjee et al. 2001; Roberts & Wintle 2001) in an attempt to minimise the contribution of feldspar-derived luminescence signals for D_e measurement. This variant of the SAR protocol consists of two signal readout steps after regenerative and test dose irradiation, with firstly an IR stimulation to reduce part of the feldspar signal, and secondly a blue stimulation aimed at releasing the quartz signal. The suitability of this protocol was checked using performance tests such as preheat plateau tests (PPT) and dose recovery tests (DRT). For the PPT applied to the quartz fraction, the D_e was measured for preheat temperatures in the range of 180-260°C (in 20°C increments) with a constant cutheat prior to a test dose readout of 160°C. DRT included a 3 h bleach with an Osram Duluxstar 24 W/827 lamp to bleach the natural signal, followed by β-irradiation with a dose in the order of the expected natural dose. The D_e was then determined for identical preheat conditions as for the PPT.

The procedure for D_e determination on the polymineral fraction followed a "normal" SAR protocol with experimental parameters, as specified in the supplementary materials. In order to account for the effect of anomalous fading, storage tests were used to estimate the amount of signal loss over time, and the polymineral ages were fading-corrected according to the approach by Huntley and Lamothe (2001). Equivalent doses of individual aliquots were determined using the Analyst software (Version 4.31.9; Duller 2015); the final D_e estimate for all samples was calculated using the Central Age Model (CAM; Galbraith et al. 1999) as implemented in the function calc_CentralDose) in the R (R Core Team 2021) package 'Luminescence' (v0.8; Kreuzer et al. 2012, 2021).

In order to assess the environmental dose rate, surrounding sediment samples were milled to grain sizes <63 µm and analysed by α-counting (U, Th; Aitken 1985) and ICP-OES (K). The estimated water content includes an additional uncertainty of (absolute) 5 % to account for moisture fluctuations during burial time. Dose rates and ages were calculated using DRAC (v1.2; Durcan et al. 2015) and considering the conversion factors of Guérin et al. (2011), α-attenuation factors of Brennan et al. (1991) and β-attenuation factors of Guérin et al. (2012).

Results

Results from the geophysical prospections

The rough ground of the ploughed and sloped field meant that the geomagnetic mapping was quite disturbed, visible by linear disturbances especially in the eastern part of the survey (Fig. 6). Further issues included: the high number of dipoles, probably

showing modern scrap metal and some anomalies with low values (<15 nT) in the southern field. One of these, visible as an anomaly with $\sim+11$ nT and 2-meter diameter, was located at the periphery of Area 6K and was excavated by Trench 4. It revealed a clear feature, possibly from the Bronze Age, showing a Holocene colluvium of >2.5 m depth.

The resistivity section for the ERT-profile (Fig. 7) generally shows three main units with different ranges of resistivity. The total values range only between 10 to $40 \Omega\text{m}$, but in comparison an agreement with the drilling results, the relative differences can be attributed to different substrates. The selected data provides depth information up to approximately 7-8 m. The lowermost unit demonstrates electrical resistivity between 10 and $20 \Omega\text{m}$ and represents the weathered bedrock (Kandern formation, blue and turquoise colors), showing very low electrical resistivity values due to the high conductivity of the clayey marly limestone. On the upslope (left), this unit starts at a depth of 1-2 m and drops significantly from about 15 m distance down the slope. Further downslope, it appears at an increased depth of 3-4 m. Where the strata of the Kandern Formation are close to the surface, it correlates with the area where most surface finds occur (Area A). Here, former archaeological layers with objects in situ have been destroyed or redeposited. A second main unit ranges between 20 and $30 \Omega\text{m}$ (green colors to yellow colors) and occurs between an 18 to 35 m horizontal distance at depths

of about 1 to 3.5 m. It stands for older loess deposits, which are partly decalcified, particularly where the supposed paleosoils are located (yellow color). Paleosoils (Units 4, comp. Fig. 5), loam loess (Unit 5) and silty loam with ore beans (Unit 6) might be represented by resistivities around $28 \Omega\text{m}$. In comparison to the findings from the Caterpillar sections, the depression structure found there (Trenches BS2 and BS3) can also be found in the ERT data. The third unit shows electrical resistivity $>30 \Omega\text{m}$ (orange to red colors) and occurs, in addition to the superficial (plough-)layer, most notably from 35 m to 52 m, where it consists mostly of calcareous loess, and from 57 m up to 75 m. It has a thickness of up to 3.5 m and correlates with Unit 3 (upper loess fine silt, comp. Fig. 5). Strikingly, the area from Trench 8, where the layer with weathered loess and paleosoils appears close to the surface again, is also visible in the ERT profile. This area corresponds to slightly lower values around a horizontal distance of 55 m. Downslope, the resistivities increase again, which is consistent with the fact that the layers from Trench 2 also dip downslope again.

Results from the excavations

Stratigraphy

It became obvious during the first campaign that the investigation encompassed a very heterogeneous underground area, with very different stratigraphic



Fig. 6. Geomagnetic survey results of the surrounding of Area A and 6K ($-20/+20$ nT). Oriented to north.

Abb. 6. Ergebnis der geomagnetischen Messungen im Umfeld von Konzentration A und 6K ($-20/+20$ nT). Nach Norden orientiert.

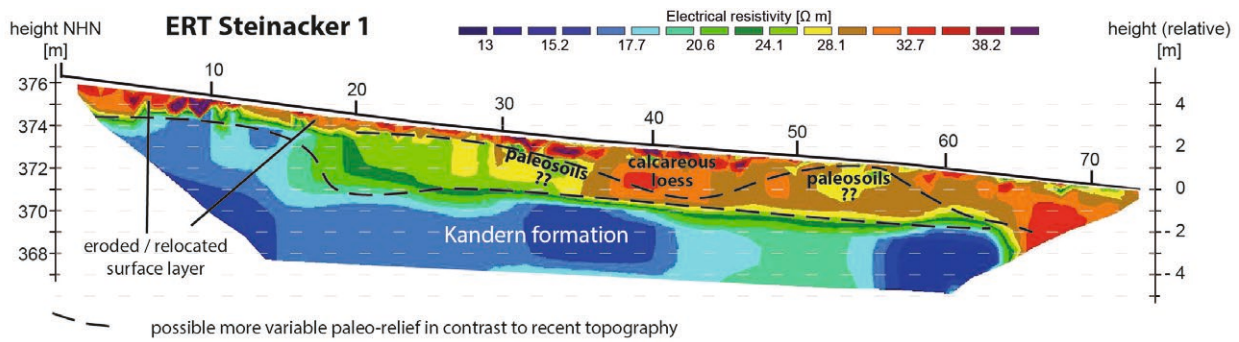


Fig. 7. The resistivity section for the ERT-profile „Steinacker“ 1. The total values range only between 10 to 40 Ωm.

Abb. 7. Widerstandsprofil der Messung „Steinacker“ 1. Die Bandbreite der Messung liegt zwischen 10 und 40 Ωm.

sequences. In 2018, most artefacts in Trench 1 appeared within the uppermost plough horizon. A second peak was visible within a sediment package of loess-loam and frost flakes at the bottom of the sequence, both separated by a nearly sterile loess package. In contrast, Trench 2 revealed a dynamic stratigraphy of sloping loess layers and paleosoils, associated with Paleolithic artefacts. In contrast again, Trench 3, some 30 m down the modern slope, revealed no artefacts and a sterile, >3.5 m thick loess package. Trench 4, excavated in the western slope at the border of Area 6K yielded at least 2.5 m of Holocene colluvium.

Thus, every documented profile demonstrated high variation in the preserved layers and their depths (Fig. 5). As we understand now, the general stratigraphy of the trenches encompasses a loess-paleosol sequence, which varies in terms of preservation due to a mixture of post-sedimentary processes from the top to the bottom and between the different areas on the slope.

The data provided by the preliminary micromorphological analysis suggests that site formation is conditioned by the interaction of both, anthropic and natural processes. Most of the stratigraphic sequence consists of sands, silts and clays, corresponding to the base sedimentation, as well as of a high content of nodules and soft masses of iron oxides. We also found, to a lesser extent, micritic accumulations of carbonates, clay illuviation and high earthworm activity. The platy structure we observed in the thin sections, however, was created by alternating freeze/thaw processes before any bioturbation activities took place. Similarly, the secondary carbonisation and clay illuviation occurred after the formation of the lenticular platy microstructure. The passage features have not been altered by the platy lenticular microstructure (Kasielke et al. 2019; Krauss et al. 2018; Kuhn et al. 2013; Lehmkuhl et al. 2016; Sauer et al. 2016). We observed a high percentage of biogenic calcite as granules of calcium carbonate in the thin sections, due to the activity of earthworms. This evidences a temperature regime with winter temperatures that allowed earthworms to survive (Krauss et al. 2018).

We detected different in situ pedogenic processes such as bioturbation (passage features and channels), clay neoformation (“stipple speckled” b-fabric) and redoximorphic activity as indicated by various kinds of nodules and hypocoatings showing irregular or diffuse outer boundaries (Kasielke et al. 2019; Krauss et al. 2018; Kuhn et al. 2013; Lehmkuhl et al. 2016; Sauer et al. 2016). The hydromorphic, edaphic and sedimentological characteristics of the sedimentary sequence are adequate to produce a large quantity of iron oxides. Finally, coarse material that has been mixed in indicates lateral transport (sheet wash) before the final deposition of the reworked loess.

At “Steinacker” the stratigraphy can roughly be subdivided into six different stratigraphic units by a macroscopic sediment classification of color and texture (Figs. 5 & 8). The most important luminescence ages related to these units are also given (for a full list see Tab. 2).

- Unit 1: Recent plough soil with a high organic content, heavily disturbed by continuous ploughing events (10YR-5/4). Not yet dated.
- Unit 2: Recent humic soil, brownish color, low clayey and silty, free of carbonates, bioturbation, high content of redoximorphic features, low content of organic material from charcoals (10YR 5-6). Not yet dated.
- Unit 3: Upper loess, yellow brownish to grey brownish in color, little bioturbation (earthworm), homogenous, fine silt, signs for cryoturbation, low content of organic material from charcoals (25Y-6/4 - 25Y-8/3), high carbonate content. 17 ± 1 ka, **fading corrected** 21 ± 2 ka (BT1818, Trench 2).
- Unit 4: Paleosoils, light to middle grey-brownish in color, homogenous, fine silt. Humified organic material, redoximorphic features, low carbonate content (10YR-5/6). 28 ± 2 ka, **fading corrected** 34 ± 3 ka (BT1911), 30 ± 2 ka, **fading corrected** 37 ± 3 ka (BT1910) both Trench 8 and 30 ± 2 ka, **fading corrected** 36 ± 3 ka (BT1682, Trench 2).
- Unit 5: Loam loess, reddish-brown to middle brown in color, silty with a low clay content, low

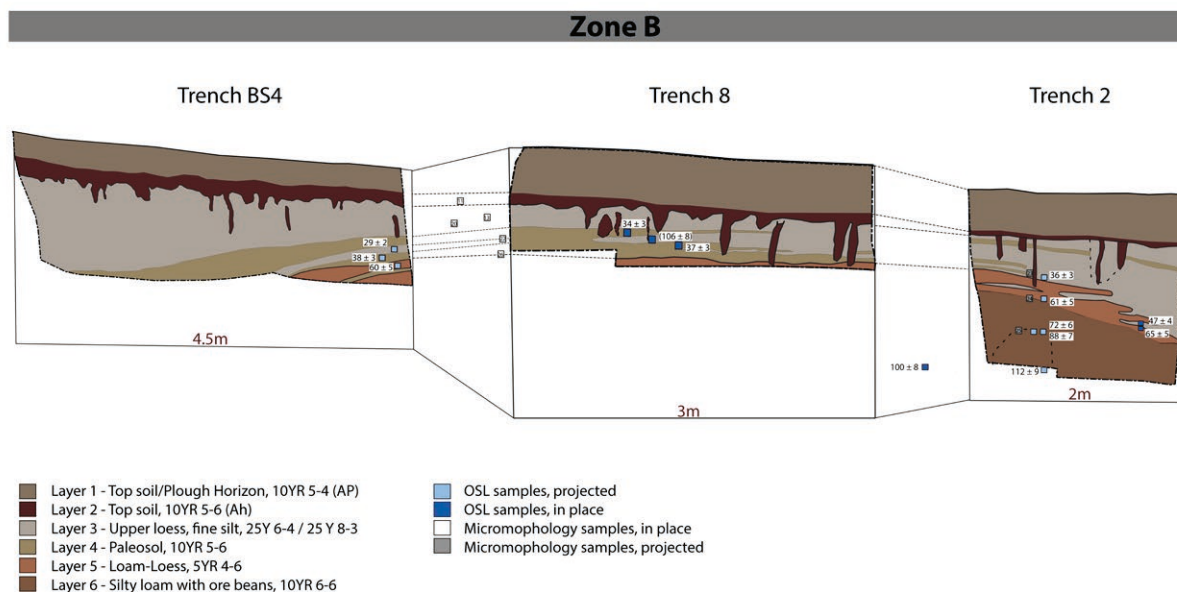


Fig. 8. Profiles of Trench 2, BS4 and 8 (direction north), showing the stratigraphic units and the location of the OSL- and Micromorphology samples.

Abb. 8. Profile der Schnitte 2, 8 und des Baggerschnitt 8 (nördliche Richtung). Visualisiert sind die stratigraphischen Einheiten und die Lokalität der OSL und Mikromorphologieproben.

carbonate content (5YR-4/6). 49 ± 4 ka, **fading corrected 60 ± 5 ka** (BT1813, Trench BS4), 50 ± 4 ka, **fading corrected 61 ± 5 ka** (BT1683, Trench 2).

Unit 6: Silty loam, middle brown in color, silty clay. Small bean ore and manganese precipitation. Small loess concretions and snails, more bioturbation (earthworm), low carbonate (10YR-6/6). 92 ± 7 ka, **fading corrected 112 ± 9 ka** (BT1686, Trench 2).

Detailed Results and interpretation of the micromorphological study

In light of the data provided by the preliminary micromorphological analysis, the on-site dynamics of formation of the documented sequence are governed by the interaction of processes of both human and natural/environmental origin, as well as post-depositional processes.

The units 3 (upper loess), 4 (paleosoils), 5 (loam loess) and 6 (silty loess) are very similar in terms of composition, groundmass, microstructure and pedofeatures (Figs. 9-11). The coarse mineral components of all thin sections are very fine quartz sand and coarse silt and clay, very well classified and quite opaque. The amount of micro-mass is very low (coarse/fine fragment ratio), and therefore, the distribution related to c/f is close to porphyric and monic. The micro-mass is a dark brown mixture of fine silt and clay, and the stipple-speckled b-fabric. The microstructure is characterised by very weakly separated subangular blocks and platy lenticular, intra-aggregate microstructure (some due to bioturbation activity). The organic components are based

on a very few micro-charcoal fragments (Fig. 9: A-B) and dark brown, humified organic pseudomorphic material (Figs. 9: C-F, 10: A-F & 11: A-D).

All samples from units 3 to 6 are characterized as followed:

1. All samples indicate edaphic traits and characteristic pedofeatures of soils with water accumulations and hydromorphy, in a seasonal way. These are soils whose main components are sands, silts and clays, and including clay illuviation (clay decantation), nodules and soft masses of iron and fragments of microcharcoals and humic pseudomorphic organic material.
2. We also detected a series of redoximorphic features: nodules (some of which have typical concretions with visible concentric layers) and soft iron masses. The redoximorphic characteristics associated with weathering are the result of alternating periods of reduction and oxidation of iron compounds in the soil (Bohn 1971; Brewer 1964). We can therefore say that there may be features of pseudogleyization. Traits that can be formed by temporary water input from seasonal oscillations that reach the lower levels of the soil or from hanging layers of water derived from water, when infiltrating the soil, are retained in the most clayey horizons (Bohn 1971; Brewer 1964).
3. The clay illuviation process is represented by the mechanical migration of the clays from the superficial to the deep horizons of the profile. Because water precipitates and infiltrates the soil, the clay from the upper horizons is mobilized, and passes into the soil solution in the form of suspension. Periodically oriented clay films are formed

Sample ID	Field code	Mineral	N	Recycling Ratio	Recuperation (%)	CAM/De (Cy/a)	U (ppm)	Th (ppm)	K (wt%)	Water content (wt%)	Dose rate (Gy ka ⁻¹)	Age (ka)	Fading-corrected age (ka)
BT1680	F1-160	PM	15	0.99 ± 0.01	1.46 ± 0.04	405 ± 13	3.74 ± 0.31	10.66 ± 1.03	1.51 ± 0.15	20 ± 5	3.87 ± 0.25	105 ± 8	127 ± 10
BT1682	F2-100	PM	6	1.02 ± 0.01	2.06 ± 0.05	119 ± 4	4.27 ± 0.31	9.59 ± 1.01	1.29 ± 0.13	14 ± 5	4.01 ± 0.27	30 ± 2	36 ± 3
BT1683	F2-120	PM	12	1.01 ± 0.01	1.76 ± 0.06	186 ± 6	3.49 ± 0.30	9.95 ± 0.99	1.30 ± 0.13	15 ± 5	3.72 ± 0.25	50 ± 4	61 ± 5
BT1684	F2-140/1	PM	11	1.00 ± 0.01	1.63 ± 0.05	217 ± 7	3.63 ± 0.43	9.44 ± 1.43	1.46 ± 0.15	20 ± 5	3.67 ± 0.26	59 ± 5	72 ± 6
BT1685	F2/140/2	PM	12	1.00 ± 0.01	1.57 ± 0.04	269 ± 9	3.41 ± 0.46	10.86 ± 1.52	1.46 ± 0.15	21 ± 5	3.70 ± 0.26	73 ± 6	88 ± 7
BT1686	F2-163	Q	10	1.02 ± 0.02	0.00 ± 0.00	330 ± 11	3.41 ± 0.46	10.86 ± 1.52	1.46 ± 0.15	21 ± 5	3.70 ± 0.26	89 ± 7	—
BT1813	OS1	PM	12	0.99 ± 0.01	1.50 ± 0.04	350 ± 11	3.18 ± 0.49	12.72 ± 1.62	1.40 ± 0.14	20 ± 5	3.79 ± 0.27	92 ± 7	112 ± 9
BT1814	OS2	PM	15	1.00 ± 0.01	1.76 ± 0.04	181 ± 6	4.26 ± 0.37	8.01 ± 1.23	1.40 ± 0.14	20 ± 5	3.71 ± 0.26	49 ± 4	60 ± 5
BT1815	OS3	PM	15	1.02 ± 0.02	1.93 ± 0.11	123 ± 4	4.24 ± 0.42	10.62 ± 1.39	1.40 ± 0.14	20 ± 5	3.97 ± 0.27	31 ± 2	38 ± 3
BT1816	OS4	PM	15	1.00 ± 0.01	1.84 ± 0.06	163 ± 5	3.90 ± 0.37	8.30 ± 1.22	1.19 ± 0.12	15 ± 5	3.62 ± 0.26	24 ± 2	29 ± 2
BT1817	OS5	PM	15	0.99 ± 0.02	1.66 ± 0.07	227 ± 7	3.71 ± 0.29	9.42 ± 0.97	1.37 ± 0.14	20 ± 5	3.63 ± 0.24	45 ± 3	55 ± 4
BT1818	OS6	PM	15	1.02 ± 0.01	2.33 ± 0.08	64 ± 2	3.85 ± 0.28	8.58 ± 0.93	1.22 ± 0.12	15 ± 5	3.89 ± 0.25	58 ± 4	72 ± 5
BT1903	S2-P1	PM	15	1.03 ± 0.01	2.47 ± 0.08	85 ± 3	4.32 ± 0.25	8.41 ± 0.84	1.29 ± 0.13	19 ± 5	3.70 ± 0.25	23 ± 2	27 ± 2b
BT1904	S2-P2	PM	12	1.00 ± 0.01	1.58 ± 0.05	240 ± 8	3.07 ± 0.21	10.04 ± 0.68	1.45 ± 0.15	17 ± 5	3.64 ± 0.23	66 ± 5	81 ± 6
BT1905	S2-P3	PM	12	1.01 ± 0.01	2.54 ± 0.09	138 ± 4	3.90 ± 0.28	8.95 ± 1.05	1.28 ± 0.13	19 ± 5	3.60 ± 0.24	38 ± 3	47 ± 4
BT1906	S2-P4	PM	16	1.00 ± 0.01	1.71 ± 0.06	200 ± 6	3.72 ± 0.38	10.54 ± 1.17	1.42 ± 0.14	20 ± 5	3.78 ± 0.25	53 ± 4	65 ± 5
BT1907	S2-P5	PM	12	1.02 ± 0.01	2.02 ± 0.08	130 ± 4	3.71 ± 0.29	10.62 ± 0.95	1.59 ± 0.16	19 ± 5	3.98 ± 0.26	33 ± 2	40 ± 3
BT1908	S2-P6	PM	12	0.99 ± 0.01	1.50 ± 0.02	304 ± 10	3.67 ± 0.29	10.54 ± 0.94	1.38 ± 0.14	20 ± 5	3.72 ± 0.24	82 ± 6	100 ± 8b
BT1909	S8-P7	PM	12	0.99 ± 0.02	1.45 ± 0.05	307 ± 10	3.94 ± 0.24	7.20 ± 0.80	1.21 ± 0.12	15 ± 5	3.54 ± 0.24	87 ± 6	106 ± 8
BT1910	S8-P8	PM	12	1.02 ± 0.02	1.95 ± 0.10	122 ± 4	4.14 ± 0.29	8.65 ± 0.95	1.48 ± 0.15	15 ± 5	4.01 ± 0.27	30 ± 2	37 ± 3
BT1911	S8-P9	PM	12	1.02 ± 0.01	2.11 ± 0.07	109 ± 3	4.41 ± 0.29	8.01 ± 0.95	1.36 ± 0.14	15 ± 5	3.94 ± 0.27	28 ± 2	34 ± 3

Tab. 2. Overview with all conducted OSL measurements.
 Tab. 2. Übersicht zu den prozessierten OSL Daten.

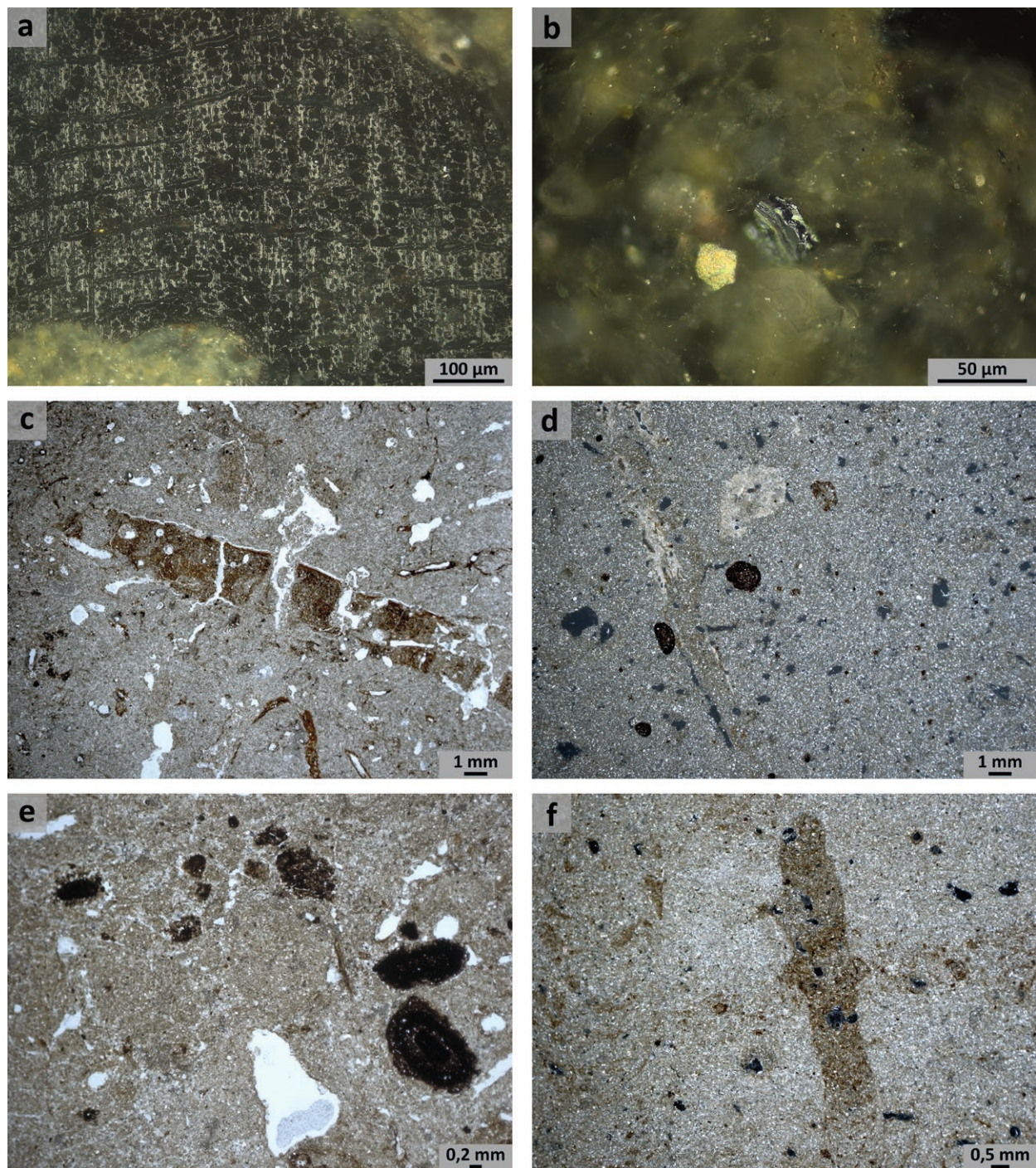


Fig. 9. Microphotographs. a) wood burned (charcoal): Detail of a fragment of charred material from wood tissue. Note the cellular structure and the strong gray color inside. Note also surrounded by an accumulation of soft mass of iron, reflected light; b) microcharcoal fragment detail, reflected light; c) reddish brown groundmass with indications of accumulation of redoximorphic substances. Stipple-speckled b-fabric dotted groundmass. The coarse / fine related distribution is porphyric to monic. The subangular blocks are present separated by channels and planes. Note clay accumulation and bioturbation activity by earthworm activity, PPL; d) view of the micritic groundmass with accumulation of orthoic and disorthoic Fe nodules in the massive microstructure, note a fragment of iron mass whose interior contains quartz grains. Also, see the different calcium carbonate accumulations (infillings and hypocoatings), XPL; e) detail of orthoic and disorthoic iron nodules, PPL and f) microcrystalline groundmass view with detail of elongated passage due to the activity of the earthworm, XPL.

Abb. 9. Mikroaufnahmen der Dünnschliffe. a) Verbranntes Holz (Holzkohle): Detail eines Fragments von verkohltem Material aus Holzgewebe. Beachte die Zellstruktur und die starke graue Farbe im Inneren. Beachte auch die Ansammlung von weichem Eisen in der Umgebung, Auflicht. b) Detail eines Mikrokohlefragmentes, Auflicht. c) Rotbraune Grundmasse mit Anzeichen einer Ansammlung von redoximorphen Substanzen. Gesprenkeltes b-Gewebe gepunktete Grundmasse. Die Korngrößenverteilung ist porphyrisch bis monisch. Die subangularen Blöcke sind durch Rinnen und Ebenen getrennt. Beachte die Tonakkumulation und die Bioturbation durch Regenwurmaktivität, PPL; d) Blick auf die mikritische Grundmasse mit Ansammlung von orthorhischen und disorthorhischen Fe-Knollen im massiven Gefüge, beachte ein Fragment der Eisenmasse, dessen Inneres Quarzkörner enthält. Man beachte auch die verschiedenen Ansammlungen von Kalziumkarbonat (Füllungen und Hypokausten), XPL; e) Detail der ortho- und disorthorhischen Eisenknollen, PPL; und f) Ansicht der mikrokristallinen Grundmasse mit Detail der durch die Aktivität des Regenwurms verlängerten Passage, XPL.

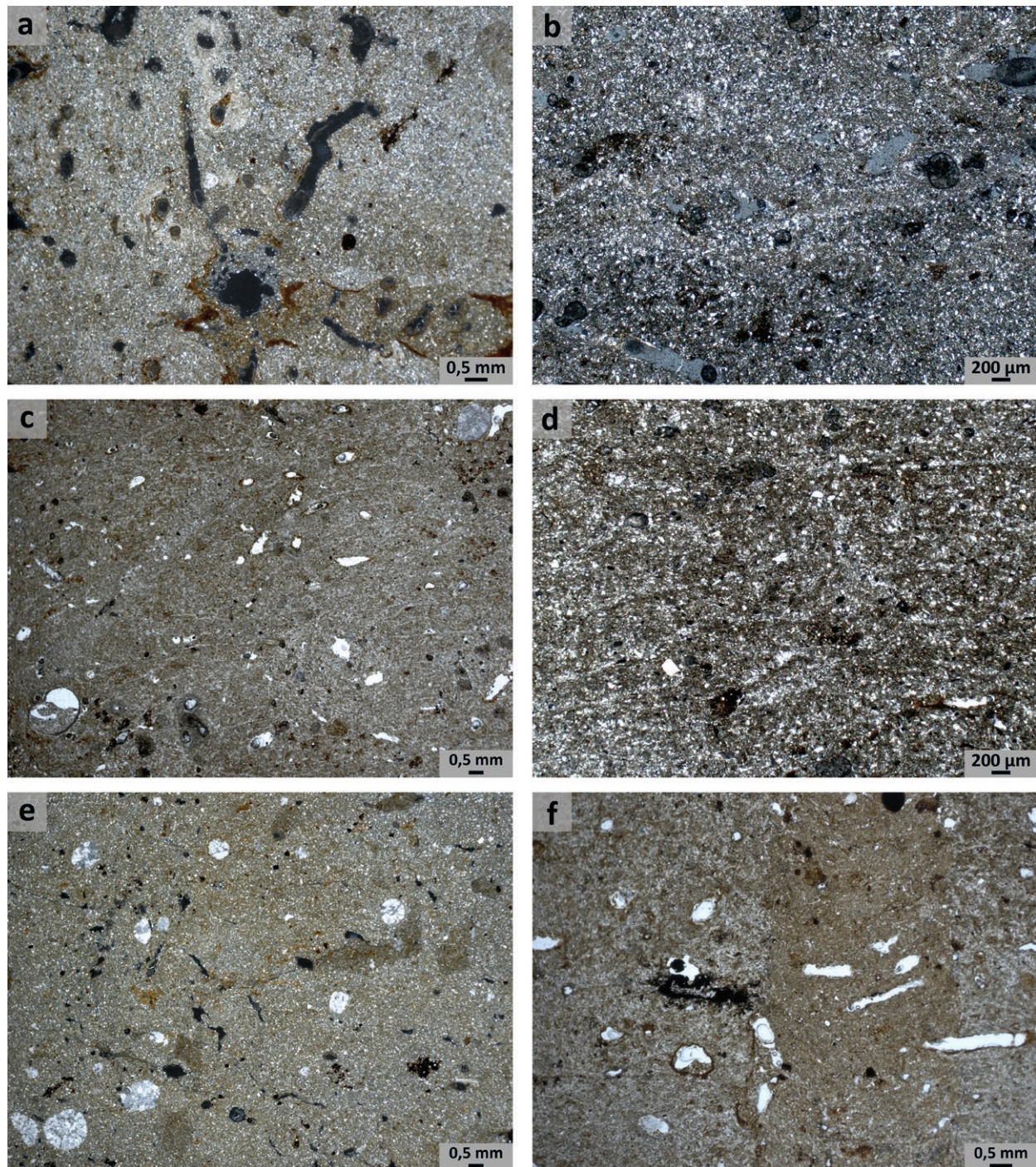


Fig. 10. Microphotographs of Samples GP 22 to GP 26: a) view of the groundmass composed of sands, silts and clays, see the accumulation of illuvial clay with dark coloration and coatings and hypocoatings of calcitic accumulation due to bioturbation activity, XPL; b), c) and d) stipple-speckled microstructure indicative of redoximorphic features. On the one hand, accumulation of orthic and disorthic nodules of Mn and Fe, micritic calcitic accumulation and organic pseudomorphous material. See c) gastropod fragment (lower left corner), b) in XPL and c) and d) in PPL; e) view of the groundmass with iron nodules, fragments of humified organic material and degraded due to iron oxide neo-formations. Note the high accumulation in the massive microstructure of biogenic calcite as granules of calcium carbonate, XPL and f) detail of passage feature due to earthworm activity: they are elongated. The worms form different semicircular and laminar shapes. Making burrows. See detail of blackish fragment of humified organic material, PPL. For the location of samples GP 22-26 see figure 8.

Abb. 10. Mikroaufnahmen der Dünnschliffe. Mikrofotografien der Proben GP 22 bis GP 26: a) Blick auf die Grundmasse aus Sanden, Schluffen und Tonen; man erkennt die Anhäufung illuvialen Tons mit dunkler Färbung und Überzügen und Hypokaustum von Kalzitanhäufungen aufgrund von Bioturbationstätigkeit, XPL; b), c) und d) Stippige Mikrostruktur, die auf redoximorphe Merkmale hinweist. Auf der einen Seite Anhäufung von ortho- und diorthischen Mn- und Fe-Knollen, mikritische Kalzitanhäufung und organisches pseudomorphes Material. Siehe c) Schneckenfragment (linke untere Ecke), b) in XPL und c) und d) in PPL; e) Blick auf die Grundmasse mit Eisenknollen, Fragmenten von humifiziertem organischem Material und durch Eisenoxidbildung degradiertem Material. Beachte die starke Anreicherung von biogenem Kalzit in Form von Kalziumkarbonatgranulat in der massiven Mikrostruktur, XPL und f) Detailaufnahme der Gänge, die durch die Aktivität der Regenwürmer entstanden sind: Sie sind länglich. Die Würmer bilden verschiedene halbkreisförmige und laminare Formen. Sie bauen Höhlen. Siehe Detail eines schwärzlichen Fragments von humifiziertem organischem Material, PPL. Zur Lage der Proben GP 22-26 siehe Abbildung 8.

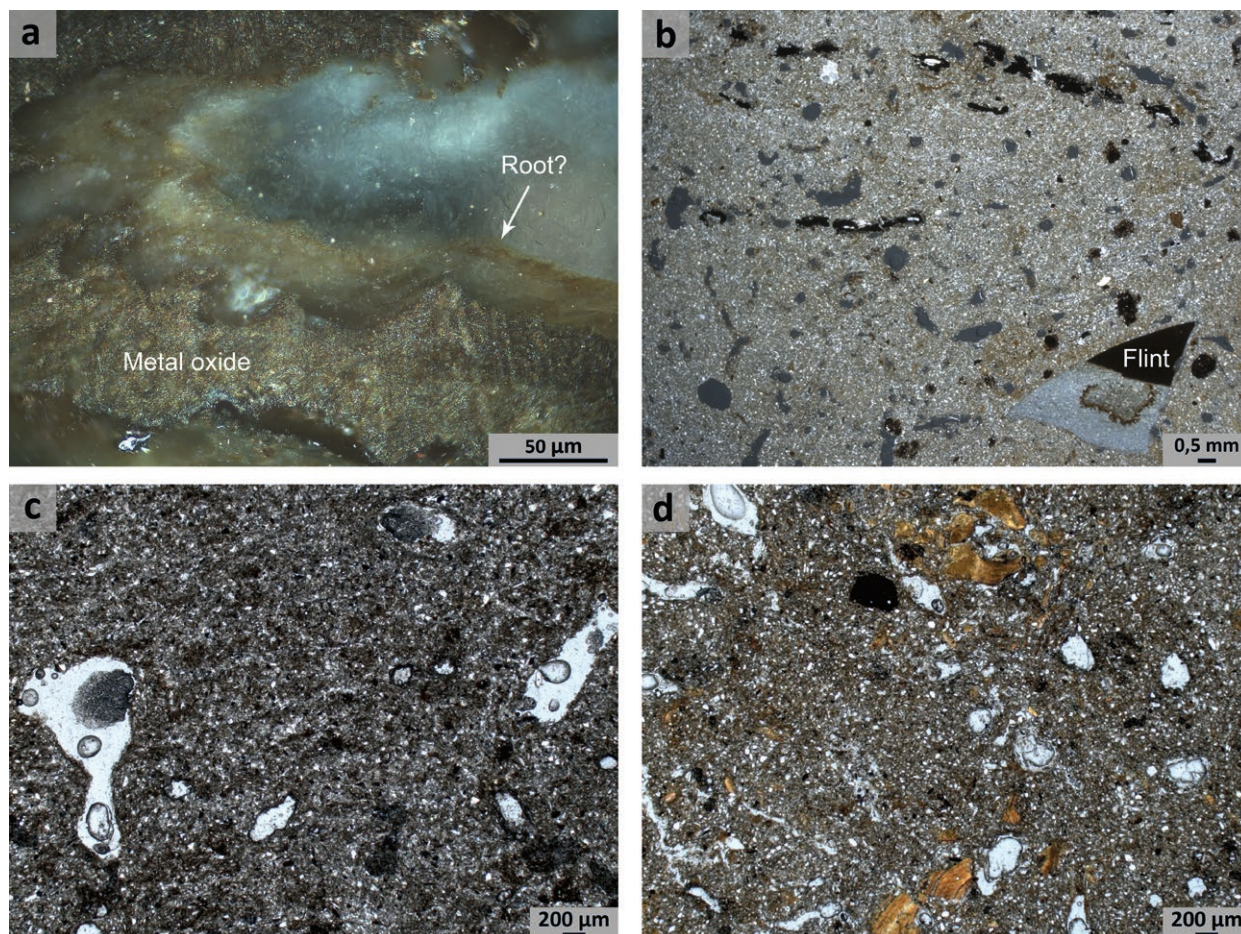


Fig. 11. Microphotographs of Sample GP 26 from trench BS4: a) detail of a possible root fragment (decomposing organic material, permineralization), indicative that iron metal oxide (blackish-grayish coloration, indicated in the image) replaces organic matter (reddish fragments, reflected light); b) detail of hydromorphic features with accumulation of iron nodules, hypocotings and accumulation of iron masses affecting the entire groundmass, detail of iron nodules and detrital humified organic material. See fragment of flint, XPL; c), view of reddish brown micromass and detail of the groundmass with indications of accumulation of redoximorphic substances. See Lenticular platy microstructure. The related coarse / fine distribution is porphyric to monic, PPL and d) detail of groundmass with accumulation of ortho- and disortho-iron nodules in the massive microstructure, note accumulation of illuviation of microlaminated clays (orange coloration and moderately anisotropic), PPL. For the location of sample GP 26 see figure 8.

Abb. 11. Mikrofotografien der Probe GP 26 aus dem Schurf BS4: a) Detail eines möglichen Wurzelfragments (zersetztes organisches Material, Permineralisierung), das darauf hindeutet, dass Eisenmetalloxid (schwarzgraue Färbung, im Bild angedeutet) organisches Material (rötliche Fragmente) ersetzt, Auflicht; b) Detail der hydromorphen Merkmale mit Anhäufung von Eisenknollen, Hypocoats und Anhäufung von Eisenmassen, die die gesamte Bodenmasse betreffen, Detail von Eisenknollen und detritischem humifiziertem organischem Material. Siehe Feuersteinfragment, XPL; c), Ansicht der rotbraunen Mikromasse und Detail der Grundmasse mit Anzeichen der Anreicherung von redoximorphen Substanzen. Siehe lenticuläre Plattenstruktur. Die zugehörige Grob-/Feinverteilung ist porphyrisch bis monisch, PPL, und d) Detail der Grundmasse mit Anreicherung von ortho- und disortho-Eisenknollen im massiven Gefüge, beachte die Anreicherung von mikrolaminieren Tonen (orange Färbung und mäßige Anisotropie), PPL. Zur Lage der Probe GP 26 siehe Abbildung 8.

- increasingly thicker, showing a strong shine (clay cutans; Dorronsoro & Aguilar 1988; Fedoroff 1973; Fedoroff et al. 2010; Mckeague et al. 1980).
4. Charcoals and humidified material: The alteration observed in the carbonaceous fragments is mainly a mechanical alteration by oxidation, and hypocotings of the carbonaceous material. Metal oxide replaces organic matter. We identified "humidified plant material" that appeared prior to combustion, such as charcoals, that are not really the result of combustion activities. It appears with a blackish and undone coloration (Fitzpatrick 1984). This is due to the humidity of the environment and the continual processes of reduction and oxidation.

5. Numerous passages resulting from earthworm activity could be documented. The worms form different semi-circular and laminar shapes. The dark vertical streaks representing permanent burrows are only visible in subsoils due to colour contrast. In Europe, these deeper burrows mostly belong to *Lumbricus terrestris*. Calcite infillings and coatings are due to roots and earthworms. There is biogenic calcite, making granules of calcium carbonate (Barthod et al. 2020; Canti 2003).

An age model based on luminescence dating

Figure 12 shows typical OSL and IRSL decay curves, as well as a typical IRSL dose-response curve (see also Tab. 2). Based on the PPT and DRT, a preheat

temperature of 240°C was chosen for subsequent quartz measurements. In general, the applied protocol seems to be successful in recovering known doses for preheat temperatures in the range 180-240°C.

The dose-response curves obtained for all polymineral measurements can be considered to be in the linear range; those of the quartz measurements are well below the $2D_0$ threshold, usually taken as an upper limit for reliable dose estimation (Wintle & Murray 2006). Storage tests for two polymineral samples gave

g -values of 1.86 ± 0.07 %/decade (BT1903; $N = 4$) and 2.28 ± 0.24 %/decade (BT1908; $N = 3$). Since these values overlap at 2σ , an averaged g -value of 2.07 ± 0.21 %/decade was adopted to correct all other samples for fading. The results of the luminescence measurements and dose rate assessment are summarised in table 2.

The final IRSL ages span the range from ~20 ka to ~130 ka and demonstrate that the upper 2 m of the sedimentary sequence at the area of investigation

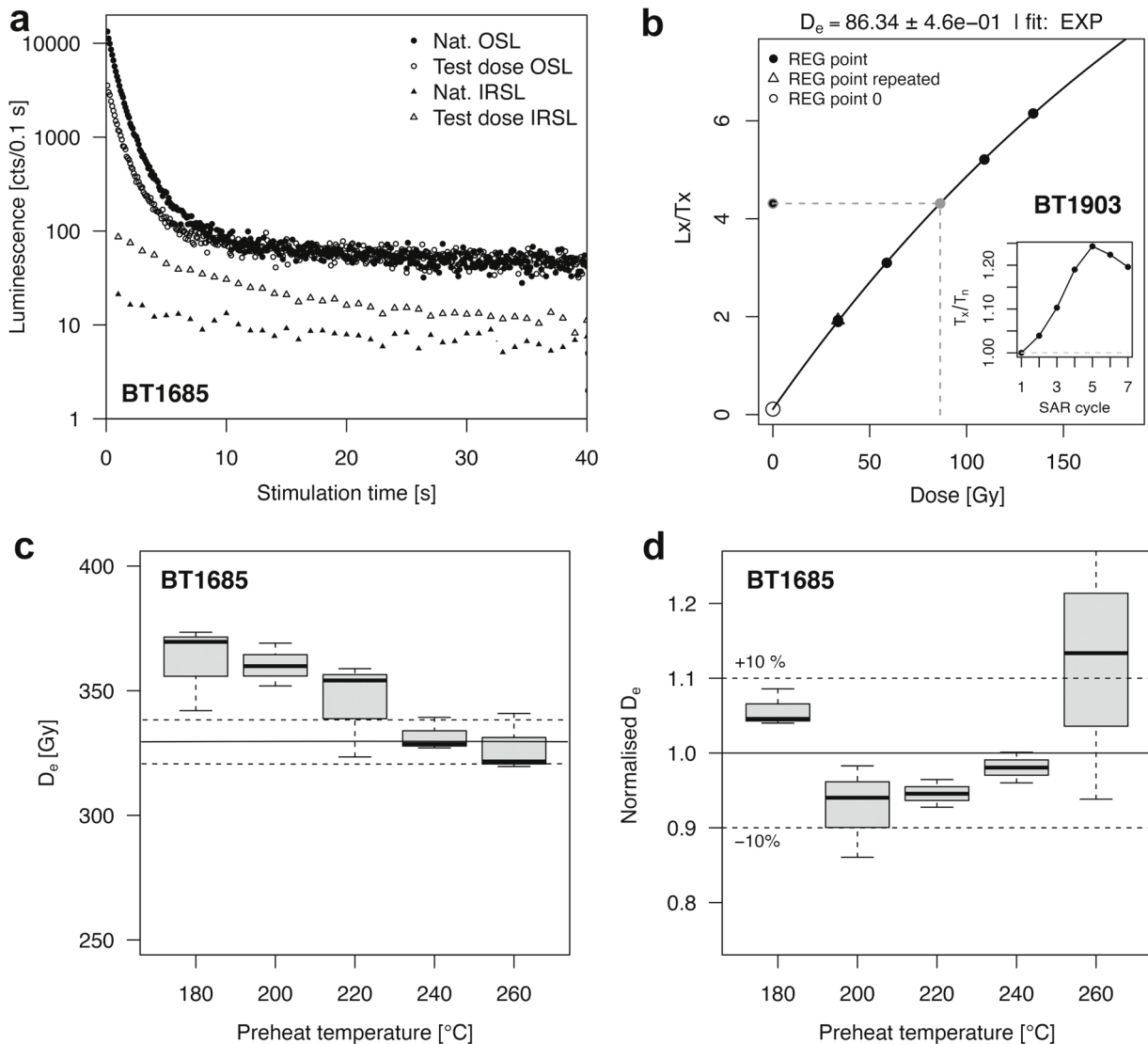


Fig. 12. a) Typical OSL and IRSL decay curves of sample BT1685, the sample with the least feldspar contamination in the quartz fraction; b) Typical dose-response curve for one aliquot of polymineral sample BT1903. The inset shows the normalized change in sensitivity in the course of the SAR protocol; c) Results of the preheat plateau test for the quartz fraction of sample BT1685, shown as boxplot. Three aliquots were measured for each preheat temperature. The solid line indicates the mean dose obtained for preheat temperatures of 240°C and 260°C, the dashed lines the corresponding standard deviation at 1σ and d) Results of the dose recovery test for the quartz fraction of sample BT1685, shown as boxplot. Three aliquots were measured for each preheat temperature and the recovery dose was ~300 Gy.

Abb. 12. a) Typische OSL- und IRSL-Ausleuchtcurven der Probe BT1685, der Probe mit der geringsten Feldspatkontamination in der Quarzfraktion; b) Typische Wachstumskurve für ein Aliquot der polymineralischen Probe BT1903. Die kleine Abbildung zeigt die normalisierte Änderung der Lumineszenz-Sensitivität im Verlauf des SAR-Protokolls; c) Ergebnisse des Vorheiz-Plateau-Tests für die Quarzfraktion der Probe BT1685, dargestellt als Boxplot. Für jede Vorheiztemperatur wurden drei Aliquots gemessen. Die durchgezogene Linie gibt die mittlere Dosis an, die bei Vorheiztemperaturen von 240°C und 260°C erzielt wurde, die gestrichelten Linien die entsprechende 1σ -Standardabweichung und d) Ergebnisse des Dose Recovery-Tests für die Quarzfraktion der Probe BT1685, dargestellt als Boxplot. Für jede Vorheiztemperatur wurden drei Aliquots gemessen, und die gegebene Dosis betrug ~300 Gy.

witnessed an entire glacial-interglacial cycle. The fact that the OSL ages are statistically indistinguishable at 1σ from the fading-corrected IRSL ages gives confidence in the accuracy of the latter. It must be noted, however, that the quartz fine grain ages correspond to a dose range in which dose underestimation has been observed (e.g., Trandafir et al. 2015). It therefore cannot be excluded that both quartz and polymineral ages suffer similarly from age underestimation. On the other hand, partial bleaching that might have occurred during sediment re-working and re-location – especially during times with strong periglacial processes – cannot be clearly traced with the fine grain dating methodology. Analyses of sand-sized (single) grains could add another dimension to interpreting site-formation from a chronological viewpoint. Nevertheless, the luminescence samples provide a first framework for the age of the different stratigraphic units and the human activities therein, which will be presented in more detail in the following sub-chapters. Thereby the site was separated into the uppermost Zone A, encompassing the surface concentration of area A and Trenches 1, BS1, BS2 and BS3 (Figs. 2, 4 & 5) and the lower Zone B around the Trenches 2,6, 8, 9 and BS4.

Synthesis for Zone A

Zone A encompasses the main surface artefact scatter documented over the last 20 years (Fig. 4: Area A), Trench 1 and the north-west part of the Caterpillar Trench BS1 (Fig. 5). Both profiles show the continuous destruction of the upper horizons by ploughing and other processes, which matches the observations from the ERT measurements. While the uppermost Pleistocene activities seem to be lost or strongly disturbed, the lowermost part of the stratigraphy contains interesting features regarding human activities and radiometric dating.

Zone A includes unit 1 (plough horizon), of 30 cm thickness, which encompasses some relocated UP artefacts, as well as modern pottery and metal objects. Below that is an 85 cm thick package of archaeologically sterile and eroded loess, followed by Unit 6, a loam-loess with a high percentage of frost shatter and iron ore beans. From the archaeological point of view, only the lowermost part of Unit 6 is of interest. It seems to be undisturbed regarding the many intact earthworm channels identified within the thin sections (Fig. 10: f). The only IRSL date for Unit 6 in Trench 1 provides an interglacial age of 127 ± 10 ka (fading-corrected, BT1680).

Lithic assemblage

There are numerous surface finds from surface concentration A, with an estimated number of >6,000 artefacts from the two collectors F. Gröteke and G. Lang alone. As the area is still continually surveyed by amateur archaeologists, and also looters, the overall number will be much higher. Tanged points, several

gravette- and microgravette implements, burins, endscrapers and a few laterally retouched artefacts also belong to this concentration (cf. Braun 2015) and support its dating to the Gravettian. Since we did not have an opportunity to evaluate the surface collections as a whole, and the assemblage composition is affected by the selection criteria of the corresponding collectors, this remains subject to future research. However, a first look fits very well with the information at hand from Mähling's surface collection (Pasda 1998).

The surface assemblage mainly consists of unretouched blades and bladelets, as well as some flakes and the presence of fragments of blade cores (Fig. 13: 1) and crested blades (Fig. 13: 2) implicates (laminar) blank production on-site.

Lithics from the excavated assemblage of Zone A (N = 1,104, mainly Trench 1, see Tab. 1) are also almost exclusively made of "Bohnerzhornstein Type Rauracien" (>95%; N = 1,065). While complete artefacts are very rare, the state of conservation can be considered good, with a low proportion of patinated finds and rounded edges. Pseudoretouches are common in the upper part of the stratigraphy, and lateral damage that can be traced to modern agricultural activities. Many pieces also display signs of frost damage, while burnt artefacts are very rare (<1%) (Tab. 3). The middle section of the sequence is nearly sterile from an archaeological point of view.

The number of chunks and pseudo-artefacts, presumably created by thermal phenomena (mainly frost), reaches its peak in the lowest artificial layers 6 & 7 with 89.5% (see Tab. 4). In contrast, chunks are only represented by 8.8% in the layers above. Thereby the following definition was used:

- Knapped lithic remains show clear features of knapping (ventral and dorsal sides, butts, signs of percussion like bulbs etc.).
- Thermal scatter: show no features of knapping, but only surfaces that can be characterized as thermal domes.
- Other: no thermal domes, but also no clear features of knapping and/or signs of percussion.

The typological/technological spectrum in the uppermost unit consists of five intentionally modified pieces (one endscraper, one sidescraper, two irregular lateral retouches and one potential fragment of a Font-Robert point (Fig. 13). Several burin spalls and crested blades demonstrate tool production and maintenance on-site. The unmodified artefacts consist of a few fragments of blades/bladelets, and several flakes/knapping debris. Only a small number of finds are considered clear artefacts in the lower units, and only one shows retouch.

The preliminary use-wear analysis conducted on 147 sampled pieces (Tab. 5) from Trenches 1, 2 and 6 has shown that eight artefacts (5.4%) display evident micro traces of use, all from the lower part of Trench 1. Two artefacts might display signs of former usage,

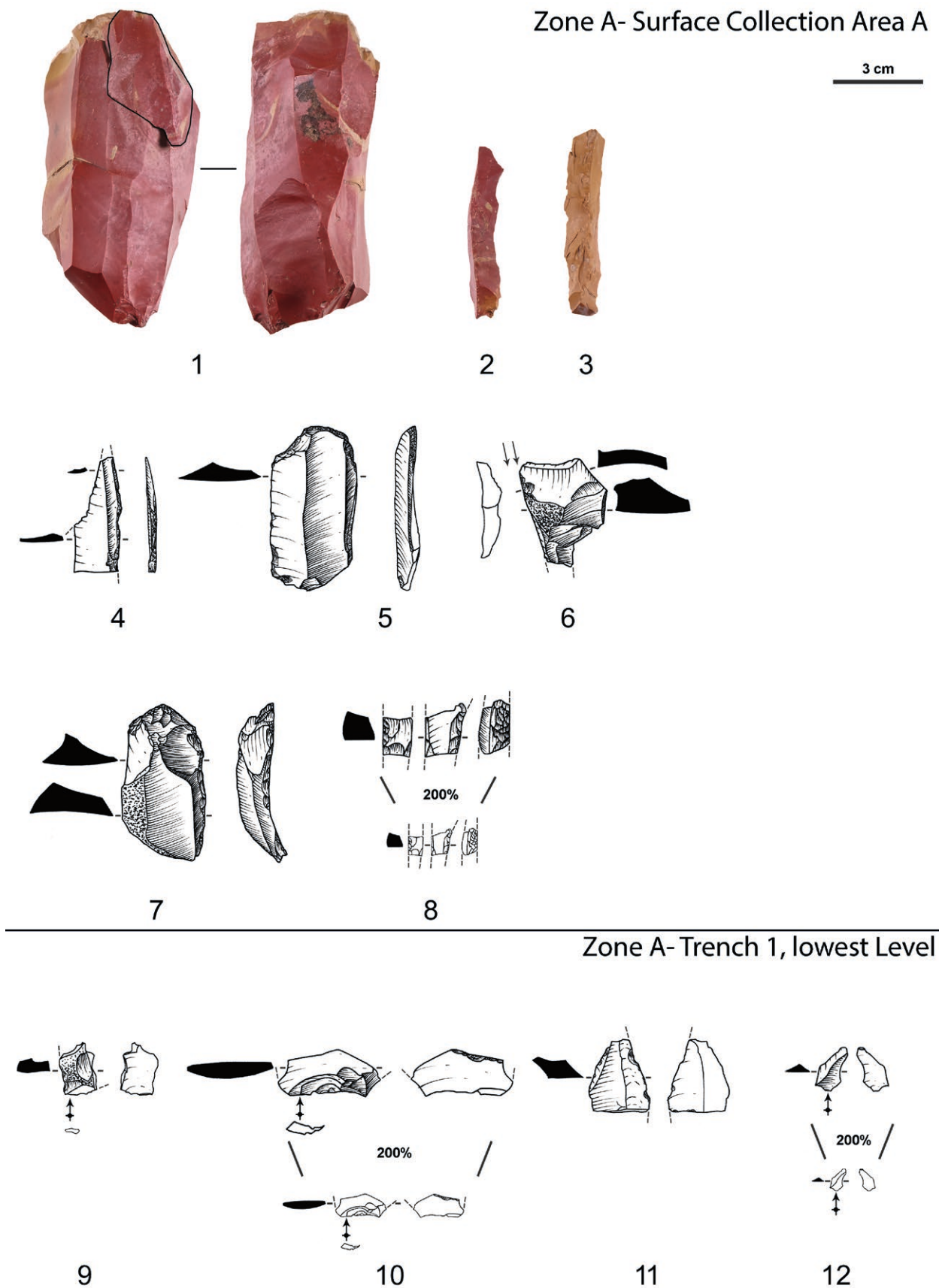


Fig. 13. Artefacts from Zone A. 1 Bidirectional blade core, 2-3 crested blade, 4 partially backed blade, 5 shouldered endscraper, 6 Burin on natural plane, 7 Endscraper with unilateral retouch, 8 possible peduncle fragment of a Font-Robert point, 9, 11-12 Knapping debris, 10 small flake. Photos by M. Bradtmöller, Illustrations by A. Calvo.

Abb. 13. Artefakte von Zone A. 1 Bidirektionaler Klingenkern, 2-3 Kerkkantenklingen, 4 partiell rückengestumpfte Klinge, Kratzer, Stichel an natürlicher Fläche, Endretusche mit unilateraler Retusche, 8 vermeintliches Stielfragment einer Font-Robert Spitze, 9, 11-12 Absplisse, 10 kleiner Abschlag.

Modified pieces	N	%
No thermal alteration	350	31.8
Alteration by frost	740	67.3
Alteration by heat	2	0.2
Indet	7	0.6
Total	1,099	100.0

Tab. 3. Trench 1. Proportion of pieces modified by frost or heat.

Tab. 3. Schnitt 1. Anteil der lithischen Stücke mit Frost oder Hitzeeinwirkung.

that are not documentable due to preservation. All belong to lithics of the "Bohnerzhornstein Type Rauracien" recovered in Unit A6, dated to >100 ka. Interestingly, none of these is a knapped artefact, but rather the result of thermal pressure (e.g. frost). From a morphological point of view, those pieces roughly match forms regularly found among artefact assemblages, while lacking any signs of knapping or other intentional modification. There is quite high variation in form and size among the pieces. Four pieces show traces associated with soft material (e.g. wood; Fig. 14) at the lateral, and in one case also in the interior part. Three pieces show clear traces of use (lateral edge), although their specific function remains largely unclear. One piece may have been used as a scraper for hide working (Fig. 15).

Synthesis for Zone B

Zone B, encompassing Trenches BS4, 2, 6, 8 and 9 can be topographically characterized as a hight with a succession of different paleosoils at the top, which becomes visible in the ERT, as well as in the profiles of the trenches (Figs. 5 & 8). This hight can be hypothetically attributed as a 10 m wide ridge running in NE-SW direction, situated between two Pleistocene periglacial channels, which were later infilled/covered with fine silt (Upper Loess). Trench 9, which is located

Layer	Knapped lithic remains		Thermal lithic remains		Other lithic remains	
	N	%	N	%	N	%
A1	161	57.3	36	4.9	4	5.1
A2	58	20.6	1	0.1	1	1.3
A3	-	-	2	0.3	-	-
A4	-	-	1	0.1	-	-
A5	5	1.8	25	3.4	3	3.8
A6	35	12.5	288	38.9	6	7.7
A7	21	7.5	374	50.5	64	82.1
NA	1	0.4	13	1.8	-	-
Total	281	100.0	740	100.0	78	100.0

Tab. 4. Trench 1. Proportion of blanks and frost shatter per layer.

Tab. 4. Schnitt 1. Anteil der lithischen Grundformen und Forstrümmen pro Abtrag.

Sampled artefacts	Yes	Uncertain	No	Total
Trench 1	8	1	114	123
Trench 2	-	1	19	20
Trench 6	-	-	4	4
Total	8	2	137	147

Tab. 5. Table of all sampled artefacts for use-wear analysis per trench.

Tab. 5. Tabelle der untersuchten Stichprobe pro Grabungsschnitt für die Gebrauchsspurenanalyse.

around 7 m from Trench 8 in BE-direction, confirms this result.

Intact (in situ) preservation for the Mid-Upper Paleolithic (Unit 4) can be documented on the top of this ridge, which is supported by the preserved earthworm channels within the thin sections of Trench 8, and the coherent IRSL dates of 34 ± 3 ka (fading corrected, BT1911) and 37 ± 3 ka (fading corrected, BT1682) within two thin layers. The old age of 106 ± 8 ka (fading corrected) for sample BT1909, bracketed between these samples, is likely due to bioturbation. An additional clue suggesting intact stratigraphic order is the horizontal inclination of the lithics (Fig. 16).

Sediment below Unit 4 was excavated solely within Trenches 2 and BS4 and provides clear hints of erosional processes. These became visible as small erosional washouts carved within older sedimentary units and are most likely caused by heavy rain on the poorly vegetated Pleistocene surface (see Fig. 17). To support this, the inclination of the lithic remains in Trench 2 show a disordered pattern. The shifted stratigraphic setup and the disordered luminescence ages also point in this direction. The luminescence ages confirm: a) the already assumed assignment of the homogenous loess of Unit 3 to the LGM, b) the appearance of at least two occupation layers from the Early Gravettian within Unit 4, and (c) the occurrence of a thick MP sediment package as Unit 5. These observations are in line with the small, but significant lithic assemblage.

Lithic assemblage

In general, the number of individual finds in Zone B (N = 887) varies largely within the different trenches (Tab. 6). The state of their conservation can be considered good, with a low proportion of patinated finds and rounded edges. Complete artefacts are rare (10.4%), burnt and/or heated artefacts practically absent (0.2%). The assemblages almost exclusively consist of "Bohnerzhornstein Type Rauracien" (>92.3%). Pseudoretouches and lateral damage is frequent, especially in the upper unit of each trench, indicating the effect of mechanical pressure from agricultural machines (ploughs etc.). The number of chunks and pseudo-artefacts presumably created by thermal phenomena (frost in most cases) is high, between

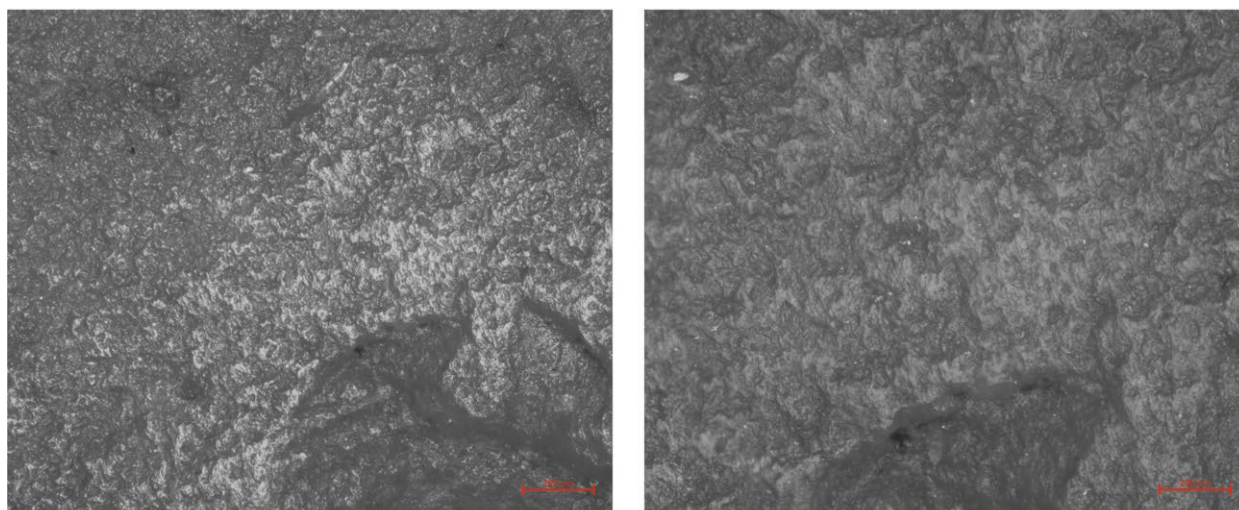


Fig. 14. Use-wear polish associated with woodworking (Artifact ID: TN-2061). Photos by J. Marreiros.

Abb. 14. Gebrauchsspuren durch Holzbearbeitung (Artefact ID: TN-2061). Fotos von J. Marreiros.

33.3% and 51.8% (Tab. 6). They are especially frequent in the lowest part of Trench 2, which reflects the observed pattern in Trench 1.

The assemblage recovered from Trenches 8 and 9 contains remnants of former knapping activity presumably in situ, aiming for the production of long regular blades/bladelets, including prismatic cores and crested blades (Fig. 18). We also identified one very small core made of lydite, which was used for the production of simple flakes, but no corresponding blanks from the same raw material. Again, we did not document any modified pieces. Trench 6 contains only a few finds, such as unretouched blanks and frost flakes, and the assemblage of Trench BS4 is affected by erosional processes. The broadest and most completely excavated Trench 2 encompasses the majority of artefacts within Zone B. Typologically, the assemblage is dominated by unmodified blanks. Among the six modified lithics there are two Middle Paleolithic

side scrapers: a simple single-edged scraper made of presumably non-local raw material, which was macroscopically identified as Chalcedon type Dinkelberg, around 30 km away from the site (M. Kaiser, personal communication), and a fragment of a transverse scraper. There are also two pieces with a lateral retouch, one with a denticulated retouch and a multitool (denticulate/scraper) not matching the definition criteria of any distinct tool types. Similar to Trenches 8 and 9, it was possible to excavate remnants of former blank/tool production, including a fragmented blade-core (accompanied by several blades), crested blades and a burin spall in the upper part of the stratigraphy. Stratigraphic Unit A7 revealed a complete Levallois core also made of non-local flint (Fig. 18: 6). Technologically corresponding flakes are missing, while there are some bigger flakes with prominent bulbs of percussion and bulbur scars. Only a few distinct MP artefacts appear in the lower part of the stratigraphy.

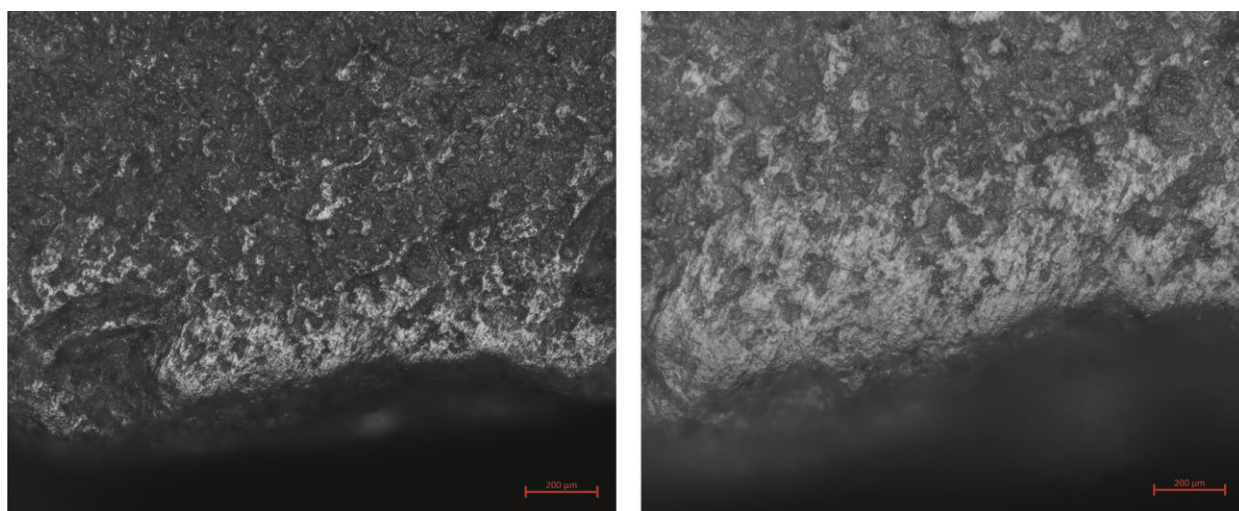


Fig. 15. Use-wear polish associated some abrasive material (e.g. hide) (Artifact ID: TN-2166). Photos by J. Marreiros.

Abb. 15. Gebrauchsspuren im Zusammenhang mit etwas abrasivem Material (vermutlich Fell) (Artefact ID: TN-2166). Fotos von J. Marreiros.

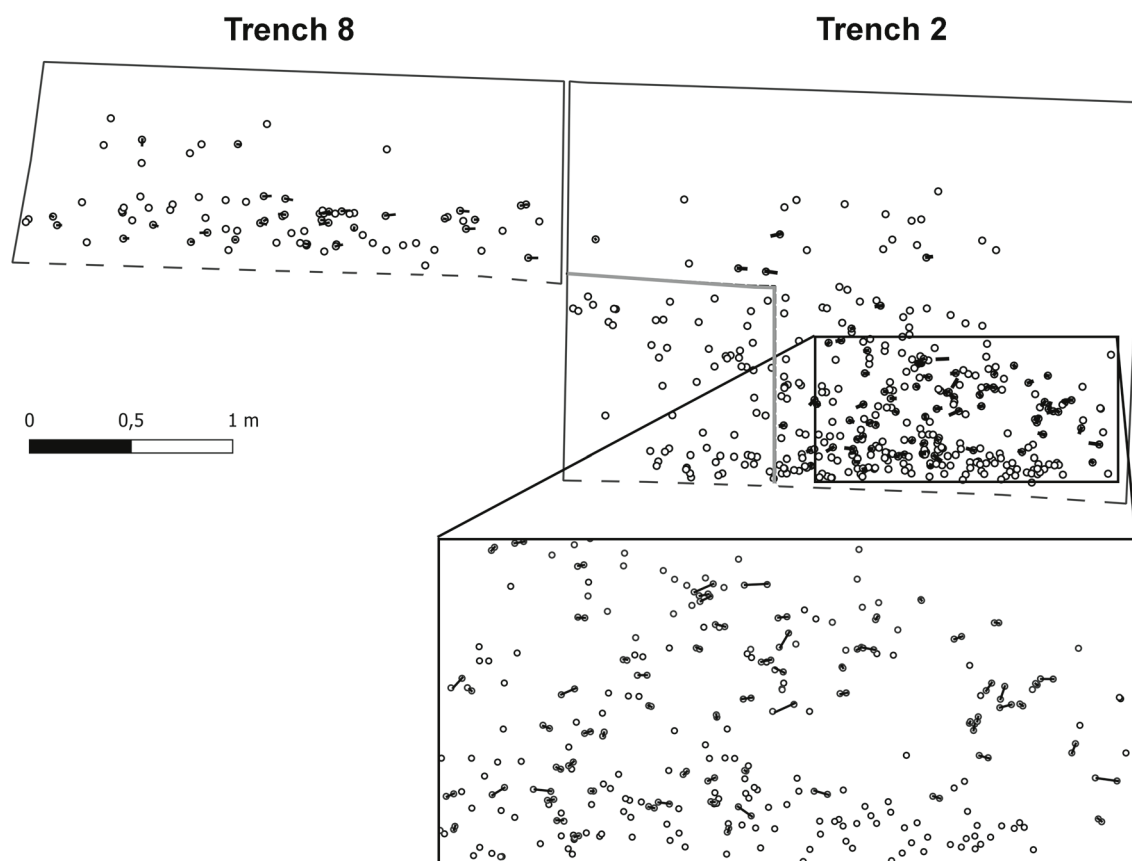


Fig. 16. Artefact plot of all pieces in Trench 2 and 8 (view to the north). Artefacts >1cm are measured with two points and showing their inclination visualized by a black line. The grey area in Trench 2 was excavated in 2018, no inclination data available here.

Abb. 16. Verteilung aller Artefakte in Schnitt 2 und 8 (Blick nach Norden). Artefakte >1cm wurden mit 2 Punkten gemessen, auf deren Grundlage die Inklination visualisiert wurde (schwarze Linie). Die grau markierte Fläche in Schnitt 2 wurde 2018 ausgegraben und noch ohne Inklination dokumentiert.

Discussion

Development of and on the slope

At "Steinacker", the Pleistocene topographic partly deviates from the current one. This indicates that the current relief is particularly influenced by modern agriculture and the associated soil erosion, a common element in loess landscapes in central Europe (Kühn et al. 2017). Not only findings of numerous artefacts in the plough horizon of the upper Zone A, but also the occurrence of calcareous loess near the surface testifies to the fact that the Late Würmian loess and the Holocene soil have been strongly eroded. Similarly, it is known from the Central European loess landscapes that a phase of landscape instability towards the end of MIS 3 may have led to severe erosion and an increased accentuation of the relief at that time (Fischer et al. 2017; Lehmkuhl et al. 2021). Multi-proxy analysis and spatio-temporal reconstruction of erosional events at the Schwalbenberg loess section (middle Rhine area) suggests pronounced erosion during the late upper Pleniglacial, channel formation and subsequent channel filling (Fischer et al. 2021). Additional erosion during the Holocene, covering the Würmian paleo-relief, is a common characteristic in loess regions,

which results in the levelling of relief and cover of the more heterogeneous Pleistocene relief, also known from south-western Germany (Kadereit et al. 2010).

Where in "Steinacker" the silty sediments have a thickness of 3-4 m above the bedrock (Kandern Formation), the corresponding layers, according to their different resistivity values, can be potentially separated into weathered loess, unweathered calcareous loess, and paleosoils. These layers occur in a very heterogeneous vertical and horizontal structure. However, even if the absolute electrical resistivity differs only slightly, the varying paleo-relief becomes partly visible. Units 4 (paleosoil), 5 (loam loess) and 6 (silty loam with ore beans), might be represented by resistivities around $28 \Omega\text{m}$ (comp. Figs. 5 & 7). In comparison to the findings from the Caterpillar sections, the depression structure found there (Trenches BS2 and BS3) can also be found in the ERT data. Unit 3, which comprises strongly calcareous loess and dates to the LGM, regarding the luminescence ages (Fig. 8). The near-surface weathered layers do not indicate recent/Holocene soil formation, but exhibit older layers exposed as the Holocene soil is completely eroded in large parts. However, in the subsurface we see a clear (linear) depression between Trenches 1 and 8 where loess from the LGM (Unit 3)

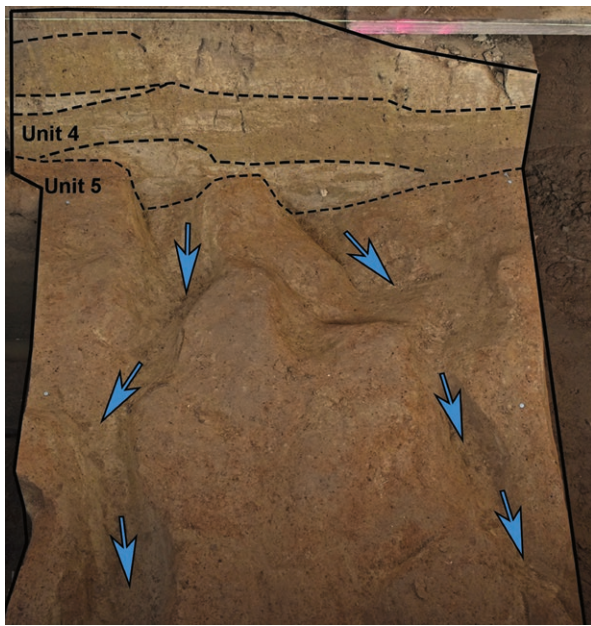


Fig. 17. Manually excavated part of trench BS4, view to the east (up the ridge). Erosional washout from fluvial dynamics, filled with sediment from Unit 4 and Upper Paleolithic artefacts.

Abb. 17. Manuell ausgegrabener Abschnitt von Baggerschnitt BS4, Blick nach Osten (den Rücken hoch). Erosionsrinne gefüllt mit Sediment von Schichtpaket 4 und jungpaläolithischen Artefakten.

is deposited (Fig. 5). The current hypothesis is that this depression, typically for loess covered slopes (comp. e.g. Fischer et al. 2021; Lehmkuhl et al. 2021), was formed before by periglacial-fluvial processes (ablation). The unweathered LGM loess is still in place within the depression, and the greater thickness in the central area indicates that the found-bearing strata are dipping with the paleo-relief here. The accentuated pre-LGM relief, the subsequent lining of the relief with loess during the LGM, and the present situation of the relatively continuous slope, makes it clear that both natural, mostly periglacial erosion and deposition processes, but also historical soil erosion, occurred spatially in a highly heterogeneous manner, and created the complex picture of the excavated sections (Fig. 19).

Chronological and functional aspects of human activities at Feldberg “Steinacker”

Located in the foothills, the lithic artefacts on a Pleistocene ridge above the small Mauchener Talmulde were generally documented at the entrance from the Rhine valley into the loess hills. The site thus encompasses several factors that favour occupation:

- 1) Assuming a predominant steppe-vegetation for the MP and UP occupation, this area was still partly sheltered from the direct impact of the Pleistocene wind from the north/northwest (van Huissteden & Pollard 2003). Paleoclimate data is scarce for this region, however.
- 2) The valley in which the open-air site is located may have served as a pathway for the movement of large ungulates such as horses, bison or reindeer, and the site itself offers a outlook down to the valley and to the region around the Hohenblauen, the highest mountain in the vicinity at 1,165 m a.s.l.
- 3) A high quality knapping material was available locally. The longer occupation history of the site can thus be explained by the possibly favourable features of the location.

According to the typological/technological analysis performed on the lithic artefacts, at least two different occupation periods can be differentiated: one for the Early Gravettian and one for the Mousterian. The Gravettian assemblage is located within Unit 4, which shows a complex stratigraphic composition of alternating loess and paleosoils. Two sub-layers could be dated to $34 \text{ ka} \pm 3 \text{ ka}$ to $37 \pm 3 \text{ ka}$ (fading corrected). The interplay of alternating loess and paleosoils in this Unit 4 thus correlate with known soil formation phases from other archives during this time (Moine et al. 2017; Fischer et al. 2021). It is therefore likely that the Gravettian occupation took place during such short interstadials as Greenland Interstadials 8 and 7, even though we cannot align our record from Steinacker to distinct soil formations as environmental proxies that correlate with high-resolution loess sections for this timespan. These dates suggest a Gravettian age which fits well with the occupations of the Swabian Jura

Lithic assemblage	Trench 2		Trench 6		Trench 8		Trench 9		BS4		Total N
	N	%	N	%	N	%	N	%	N	%	
Flakes	115	20.5	6	22.2	24	21.6	4	8.5	22	15.7	171
Small debris (<1 cm)	52	9.3	5	18.5	14	12.6	10	21.3	38	27.1	119
Blades	35	6.2	3	11.1	5	4.5	3	6.4	16	11.4	62
Bladelets	14	2.5	1	3.7	3	2.7	3	6.4	8	5.7	29
Tools	8	1.4	-	-	-	-	-	-	1	0.7	9
Cores	-	-	-	-	2	1.8	-	-	-	-	2
Thermal chunks	287	51.1	10	37.0	53	47.7	19	40.4	44	31.4	413
Others	51	9.1	-	-	10	9.0	8	17.0	11	7.9	80
Total	562	100.0	27	100.0	111	100.0	47	100.0	140	100.0	887

Tab. 6. Zone B: Overview regarding the composition of the lithic assemblage per trench.

Tab. 6. Zone B: Übersicht zur Zusammensetzung des lithischen Inventars getrennt nach Grabungsschnitten.

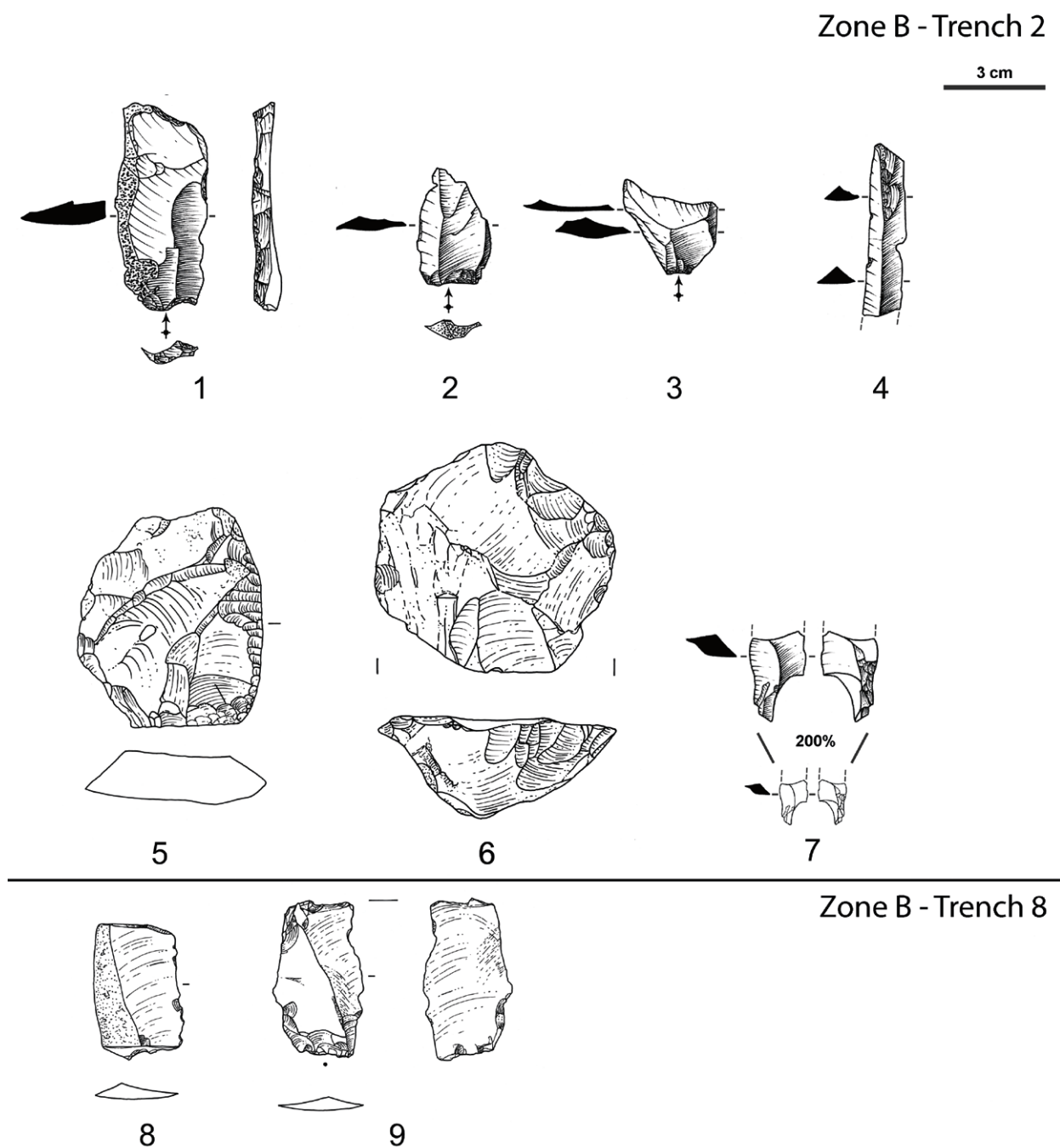


Fig. 18. Artefacts from Zone B. 1 unilateral crested blade. 2-3 Flakes, 4 core rejuvenation product, 5 Scraper, 6 Levallois core, 7 Medial fragment of a bladelet with a notch and a short bifacial retouch related to a burin-like fracture (?microburin?), 8 blade fragment with lateral edge damage, 9 blade fragment with retouch and edge damage (splintered pieces?). Illustration 1-4 & 7 by A. Calvo, 5-6 & 8-9 by Archäologische Illustrationen.

Abb. 18. Artefakte aus Zone B. 1 unilaterale Kernkanten Klinge, 2-3 Abschläge, 4 Kernverjüngungsabschlag, 5 Schaber, 6 Levallois Kern, 7 Mediales Klingensfragment (evtl. Kerbrest), 8 Klingensfragment mit Kantenbeschädigung, 9 Klingensfragment mit Retusche und Kantenbeschädigung (evtl. Ausgesplittertes Stück).

(cf. Moreau 2009; Taller & Conard 2019), yielding comparable lithic types such as Gravette points and Microgravettes, as well as Font-Robert points. Feldberg "Steinacker" and the Swabian cluster show chronological and typological similarities, although "Steinacker" is an open-air site. The lack of these is likely due to erosional and/or covering processes during the LGM (Barbieri et al. 2018, Barbieri

2019, Barbieri et al. 2021), while human occupation between ~28,000 and 16,000 BP was probably also affected by this (cf. Solich & Bradtmöller 2017). Whether this distinct time window for disturbances was also important at "Steinacker" cannot be answered properly yet. One IRSL age calculated for Unit 4 is slightly older (BT1815: fading-corrected 29 ± 2 ka). However, being derived from the flank of the

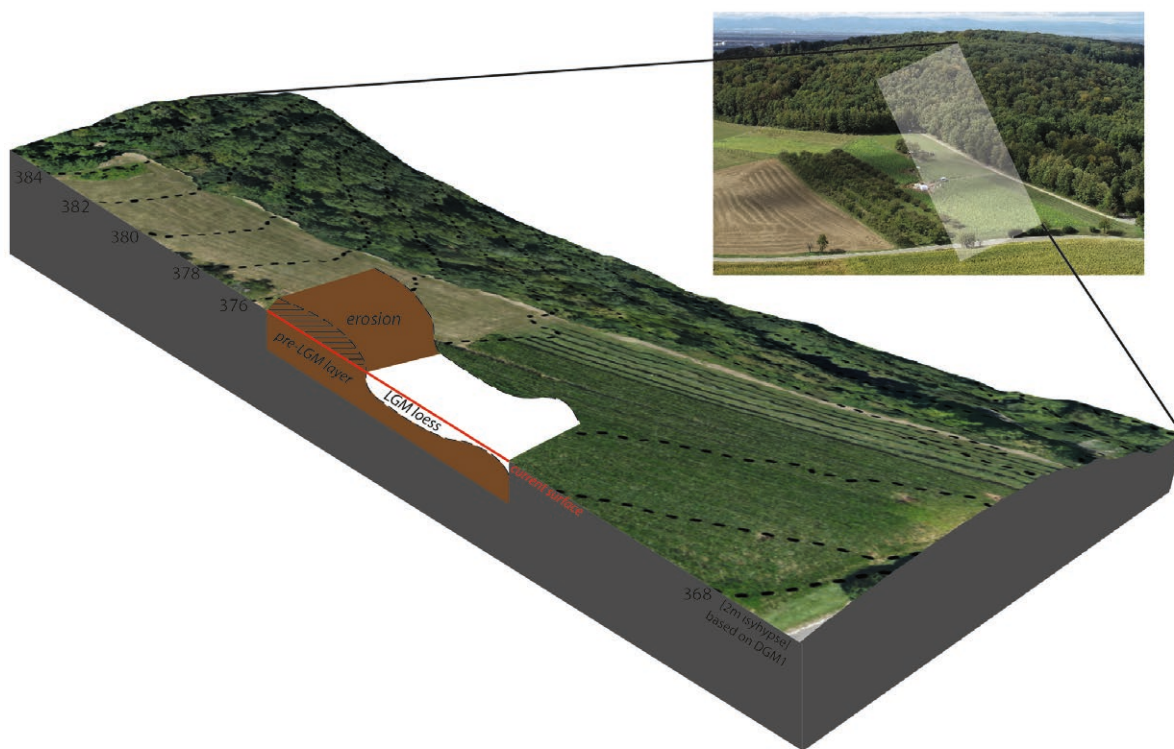


Fig. 19. Visual reconstruction of the paleo-relief under study.

Abb. 19. Visuelle Rekonstruktion des Paläoreliefs.

ridge it is possibly affected by erosion and incomplete bleaching.

On the other hand, the hypothesis of a different chronology for the major erosional processes observed at “Steinacker” would be in line with the hypothesis that erosional processes and landscape changes were out of sync in the Southern German highlands during the late Pleistocene, as suggested by Barbieri (et al. 2021, 2022).

Regarding the question of site function, it is interesting to mention that the Gravettian occupations from the Swabian Jura are showing a broader variety of residential sites and temporal camps. However, in general with a high degree of domestic activities (Moreau 2009). In contrast, the assemblage from Unit 4 at “Steinacker” can be characterised as the primary remnants of laminar blank production. Apart from a few lateral retouches, modified pieces are missing, while the in-situ character of the zones for knapping activity is perceptible in Trench 8. This composition is comparable to the results from Pasda (1998b) and Holdermann (1996) (see Tab. 6). All assemblages are showing a high number of unmodified blanks and a low number of formal tools. As an explanation, Pasda has (1998b) interpret the lithics as remnants of a workshop site for raw material acquisition and a first initialisation of cores. However, he also remarked that occupations on raw material outcrops could have produced different lithic assemblages, then on places in a distance to these (cf. Floss 1994).

Other sites from the Mid-Upper Paleolithic with a similar artefact composition and a raw material source in close vicinity are known from France and Spain. A cluster of sites near Bayonne revealed a large amount of blank production and less than 1% of tool and weapon implements (Colonge 2015). Another example is the site of Mugardua sur in the Basque Country, where primary blank production from the local, high-quality Urbasa flint and a high proportion of weapon implements (gravette points) was documented (Barandiarán et al. 2013). Both sites suggest a logistical organisation of Gravettian mobility, as assumed, for example, for sites in Bavaria (Uthmeier 2004) and Northern Spain (Bradtmöller 2014). The small amount of “Bohnerzhornstein Typ Rauracien” in Middle and Upper Paleolithic strata in the Swabian Jura possibly suggests the long-distance transport of this material (Moreau 2009), however, these pieces could also originate in higher quantity but lower quality from the Danube River (Çep 2013).

While the Upper Paleolithic component was well represented throughout the excavations, distinct Middle Paleolithic artefacts were only documented in Trench 2, which is possibly related to the shallow excavation depth within the other trenches. The Middle Paleolithic assemblage is small, and only two scrapers and one Levallois core can be technologically or typologically attributed here. In contrast to the Upper Paleolithic assemblage, which consisted almost exclusively of “Bohnerzhornstein Type Rauracien”, two

of the pieces were made of non-local raw material. Even though there are some bigger flakes with prominent bulbs of percussion and accompanying bulbous scars, they are not necessarily part of the Middle Paleolithic occupation, since they did not appear clustered and some of those pieces are also expected in an Upper Paleolithic context. We identified some scrapers in the surface collections, however, possibly in connection to the excavated Middle Paleolithic, which fit with the previously published scrapers (Braun 2008). As it stands, the Middle Paleolithic occupation is characterised by a different raw material spectrum. We assume that a small lydite core from Trench 8 might also belong to the Middle Paleolithic, and marks the beginning of corresponding Unit 5. This is also supported by a minimum IRSL age for this unit of 60 ± 5 ka (fading-corrected, BT1813).

In summary, the raw material spectrum indicates a change in site function or mobility throughout the periods. Interestingly, a changing pattern was also observed within the Bayonne cluster, which was explained by different mobility patterns (Cologne 2015). If this is also the case at "Steinacker", it can only be confirmed by comprehensive excavations of the Middle Paleolithic units. Thereby, the somehow "mysterious" traces of human activity dating to the Eemian in Trench 1 must also be considered. The assemblage from Unit 6, with a few artefacts and various frost flakes (sometimes reaching the size of 15 cm in length), is yet to be critically examined. It was probably at the upper part of the slope, which lies significantly higher due to the terrain edge observed within the ERT, that a secondary outcrop of the "Bohnerzhornstein" was accessible to the humans. The small sizes of the indisputable artefacts can be interpreted in two ways. First, they may have been washed in from upslope during erosional processes, while the frost shatter can be interpreted as a secondary deposit. Alternatively, both align with an open secondary deposit during the Eemian with the opportunistic/ad hoc use of available natural and anthropogenic blanks.

The presence of frost shatter, and especially its abundance in all areas (apart from Trench 1), is not a feature often reported from other sites. Its abundance might be explained by the hypothesis that former artefacts were fractured by frost, until the human effect was no longer visible. However, considering the quantitative relationship between frost shatter and artificial flakes, as well as their distribution among the layers at the site, we think this option is unlikely. Interestingly, traces of use-wear appeared on pieces which can safely be classified as frost-flakes. Thereby they indicate that natural flakes were intentionally used at "Steinacker" site. As use-wear traces are only visible after a long period of use for the corresponding artefact (especially when working with soft material), it is possible that larger proportions of the assemblage were used in a similar way.

Interestingly, this relationship between blanks of an unknown origin and work with soft raw material is reminiscent of the microliths from G-Layer-Complex of Sesselfelsgrotte in the Lower Altmühl Valley. Those pieces also vary in size and form, and their origin is highly debated (Freund 1968; Jöris 2003; Richter 1997). Use-wear analysis revealed a similar usage of those pieces (Lass 1994) and they neither show a dedicated place within the chaîne opératoire, nor a retouch/modification.

Conclusions

During the last four years, we have been able to gather new data for the understanding of the local paleo-relief, post-sedimentary processes, and also traces of human activities at "Steinacker" during the last 120,000 years. The complex situation discovered, however, means the analysis of important issues such as site formation, function and mobility is still at the beginning.

In the future we want to deepen the interdisciplinary cooperation already established, to further understand the local paleo-relief including underlying erosional and accumulation processes, the assemblages and their genesis. We therefore plan to expand excavation activities, further geophysical measurements, drillings and subsequent lab analyses with longer campaigns and more co-workers. It cannot be stressed enough that this has to happen in the next years. The site is in danger of losing more and more archaeological substance, and hence potential archaeological layers, which is reflected by the high number of surface finds collected by local artefact gatherers every year. Our current results also indicate that there are only a few areas left, where we can expect at least the UP horizons to remain undisturbed.

Although the Middle Paleolithic activity zone doesn't seem to be that endangered by the agricultural use of the site and erosional processes, it will be the second goal for future investigations to locate them. Identifying the used raw material sources and finding the nearby outcrops are further objectives, necessary for interpreting the site's functionality.

ACKNOWLEDGMENTS: The Department for Heritage Services Baden-Württemberg primarily funded the project, with additional funds from Rostock University. We would like to thank the Markgräfler Museum and the corresponding Work Group for Prehistory for their support during our field campaigns. Special thanks go to F. Gröteke and G. Lang for providing access to their surface collections. We are also indebted to H. Nußbaumer and U. Waldkirch, as well as the village council of Feldberg, for supporting the excavations and giving access to the "Steinacker" site, as well as the excavation team for their efforts. Finally, and importantly, we would like to express our deepest gratitude to the Warnke family for hosting the excavation team in their beautiful house. Last not least, we would also like to thank two anonymous reviewers for their comprehensive comments.

Literatur cited

- Aitken, M.J. (1985). *Thermoluminescence dating*. Academic Press, London.
- Albrecht, G. (1979). *Magdalénien-Inventare vom Petersfels. Siedlungsarchäologische Ergebnisse der Ausgrabungen 1974-1976*. Tübinger Monographien zur Urgeschichte 6. Tübingen, Verlag Archaeologica Venatoria.
- Albrecht, G. (1981). Die neuen Ausgrabungen in Munzingen 1976/77. *Archaeologica Venatoria Mitteilungsblatt* 2: 21-23.
- Albrecht, G. & Hahn, A. (1991). *Rentierjäger im Brudertal*. Führer zu archäologischen Denkmälern in Baden-Württemberg 15. Stuttgart, Konrad Theiss Verlag.
- Banerjee, D., Murray, A.S., Botter-Jensen, L. & Lang, A. (2001). Equivalent dose estimation using a single aliquot of polymineral fine grains. *Radiation Measurements* 33: 73-94.
- Barbieri, A., Leven, C., Toffolo, M.B., Hodgins, G.W., Kind, C.J., Conard, N.J. & Miller, C.E. (2018). Bridging prehistoric caves with buried landscapes in the Swabian Jura (southwestern Germany). *Quaternary International* 485: 23-43.
- Barbieri, A. (2019). *Landscape changes, cave site formation and human occupation during the Late Pleistocene: a geoarchaeological study from the Ach and Lone valleys (Swabian Jura, SW Germany)*. Universitätsbibliothek Tübingen.
- Barbieri, A., Bachofer, F., Schmaltz, E., Leven, C., Conard, N. & Miller, C.E. (2021). Interpreting gaps: A geoarchaeological point of view on the Gravettian record of Ach and Lone valleys (Swabian Jura, SW Germany). *Journal of Archaeological Science* 127: 105335.
- Barbieri, A., Maier, A., Lauer, T., Mischka, C., Hattermann, M. & Uthmeier, T. (2022). Post-LGM environments and foragers on the move: New data from the lower Altmühl Valley (Franconian Jura, SE Germany). *Journal of Human Evolution* 173: 103267.
- Barthod, J., Dignac, M.F., Le Mer G., Bottinelli, N., Watteau F., Kögel-Knabner I. & Rumpela, C. (2020). How do earthworms affect organic matter decomposition in the presence of clay-sized minerals? *Soil Biology and Biochemistry* 143: 2-10.
- Berger, G., Mulhern, P. & Huntley, D.J. (1980). Isolation of silt-sized quartz from sediments. *Ancient TL* 11: 8-9.
- Bohn, H.L. (1971). Redox potentials. *Soil Science* 112: 39-45.
- Bradtmöller, M. (2014). *Höhlenlager des Gravettien - Muster jungpaläolithischer Höhlennutzung am Beispiel des Gravettien Nordspaniens*. Hamburg.
- Barandiarán, I., Cava, A. & Aguirre, M. (2013) (Eds.). *El taller de sílex de Mugardua Sur: una ocupación de Urbasa (Navarra) durante el Gravetiense*. Universidad del País Vasco/Euskal Herriko Unibertsitatea (UPV/EHU), Leioa.
- Braun, I. (2008). Neue paläolithische Funde von Feldberg «Steinacker», Stadt Müllheim (Baden), Kreis Breisgau-Hochschwarzwald. *Archäologische Ausgrabungen in Baden-Württemberg* 2007: 25-27.
- Braun, I. (2015). The Gravettian open air site of Feldberg "Steinacker", Müllheim/Baden (Germany). *Quaternary International* 359-360: 318-323.
- Braun, I. (2021). Le site gravettien de plein air de Feldberg «Steinacker», Müllheim/Baden (Allemagne). *Paléo* 31: 76-95.
- Brennan, B.J., Lyons, R.G. & Phillips, S.W. (1991). Attenuation of alpha particle track dose for spherical grains. *International Journal of Radiation Applications and Instrumentation. Part D. Nuclear Tracks and Radiation Measurements* 18: 249-253.
- Brewer, R. (1964). *Fabric and mineral analysis of soils*. John Wiley and Sons, Nueva York.
- Bullock, P., Fédoroff, N., Jongerius, A., Stoops, G. & Tursina, T. (1985). *Handbook for soil thin section description*. Waine Research Publications, Wolverhampton.
- Canti, M.G. (2003). Earthworm Activity and Archaeological Stratigraphy: A Review of Products and Processes. *Journal of Archaeological Science* 30: 135-148.
- Courty, M. A., Goldberg, P. & Macphail, R. I. (1989). *Soils and micromorphology in archaeology*. Cambridge University Press. Academic/Plenum Publishers, New York.
- Çep, B. (2013). Ausgangsbasis oder Versorgungsstandort? Raumnutzung im Mittel- und Jungpaläolithikum des Ach- und Blautals bei Blaubeuren. *Quartär* 60: 61-83.
- Colonge, D., Claud, E., Deschamps, M., Fourloubey, C., Hernandez, M., Sellami, F., Anderson, L., Busseuil, N., Debenham, N., Garon, H. & O'Farrell, M. (2015). Preliminary results from new Paleolithic open-air sites near Bayonne (south-western France). *Quaternary International* 364: 109-125.
- Cziesla, E. (1992). *Jäger und Sammler. Die mittlere Steinzeit im Landkreise Pirmasens*. Lindencover soft, Brühl.
- Dorronsoro, C. & Aguilar, J. (1988). El proceso de iluviación de arcilla. Una revisión. *Ana. Edaf. y Agrob. XLVII*: 311-350.
- Drafehn, A., Bradtmöller, M. & Mischka, D. (2008). SDS - Systematische und digitale Erfassung von Steinartefakten. *Journal of Neolithic Archaeology* 16: 63-95.
- Duller, G.A.T. (2003). Distinguishing quartz and feldspar in single grain luminescence measurements. *Radiation Measurements* 37: 161-165.
- Durcan, J.A., King, G.E. & Duller, G. A. T. (2015). DRAC: Dose Rate and Age Calculator for trapped charge dating. *Quaternary Geochronology* 28: 54-61.
- Ecker, A. (1875). Über eine menschliche Niederlassung Aus der Rentierzeit im Löb des Rheintals bei Munzingen unweit Freiburg. *Archiv für Anthropologie* 8: 87-101.
- Ecker, A. (1877). Am Tuniberg vor langer Zeit! Ein Stückchen ältester breisgauer Geschichte. *Schau-ins-Land* 4: 89-96.
- El-Kassem, M., Bradtmöller, M. & Calvo, A. (2019). Neue Forschungen zur jungpaläolithischen Frei-landfundstelle Feldberg „Steinacker“. *Archäologische Ausgrabungen in Baden-Württemberg* 2018: 73-75.
- Fedoroff, N. (1973). The clay illuviation. In: St. Kowalinski & J. Drozd (Eds.), *Soil micromorphology*. Proc. 3rd. Int. Work. Meet. Soil Micromorphol., Wrocław, Poland, 22-28. Sept. 1969. Panstwowe Wydawnictwo Naukowe, Poland, 195-207.
- Fedoroff, N., Courty, M.-A. & Guo, Z. (2010). Paleosoils and relict soils. In: G. Stoops, V. Marcelino & F. Mees (Eds.), *Interpretation of Micromorphological Features of Soils and Regoliths*. Elsevier, Amsterdam, 623-662.
- Fischer, P., Hambach, U., Klasen, N., Schulte, P., Zeeden, C., Steining, F., Lehmkuhl, F., Gerlach, R. & Radtke, U. (2017). Landscape instability at the end of MIS 3 in western Central Europe: evidence from a multi proxy study on a Loess-Paleosol-Sequence from the eastern Lower Rhine Embayment, Germany. *Quaternary International* 502 A: 119-136.
- Fischer, P., Jöris, O., Fitzsimmons, K., Vinnepand, M., Prud'homme, C., Schulte, C., Hatté, C., Hambach, U., Lindauer, S., Zeeden, C., Peric, Z., Lehmkuhl, F., Wunderlich, T. & Wilken, D. (2021). Millennial-scale terrestrial ecosystem responses to Upper Pleistocene climatic changes: 4D-reconstruction of the Schwalbenberg Loess-Paleosol-Sequence (Middle Rhine Valley, Germany). *Catena* 196: Article-Nr. 104913.
- Fitzpatrick, E. A. (1984). *Micromorphology of Soils*. Chapman and Hall, London.
- Floss, H. (1994). *Rohmaterialversorgung im Paläolithikum des Mittelrheingebietes*. Römisch-Germanisches Zentralmuseum, Monographien Band 21. Dr. Rudolf Habelt GmbH, Bonn.
- Galbraith, R. F., Roberts, R. G., Laslett, G. M., Yoshida, H. & Olley, J. M., (1999). Optical Dating of Single and Multiple Grains of Quartz from Jinmium Rock Shelter, Northern Australia: Part I, Experimental Design and Statistical Models. *Archaeometry* 41: 339-364.
- Gersbach, E. (1969). *Urgeschichte des Hochrheins: Funde und Fundstellen in den Landkreisen Säckingen und Waldshut Bad*. Fundber. Sonderh. 11, Staatl. Amt für Ur- und Frühgeschichte, Freiburg i. Breisgau.

- Golberg, P. & Macphail, R. (2006). *Practical and Theoretical Geoarchaeology*. Blackwell Publishing, Oxford.
- Guenther, E. W. (1968). Ist die Rentierjägerstation von Munzingen ein „Löbmagdalénien“? *Quartär* 19: 93-124.
- Guérin, G., Mercier, N. & Adamic, G. (2011). Dose-rate conversion factors: update. *Ancient TL* 29: 5-8.
- Guérin, G., Mercier, N., Nathan, R., Adamic, G. & Lefrais, Y. (2012). On the use of the infinite matrix assumption and associated concepts: A critical review. *Radiation Measurements* 47: 778-785.
- Hecht, S., Mächtle, B. & Bubbenzer, O. (2022). Geoelektrische Tomographie. In: C. Stolz & C. Miller (Eds.), *Geoarchäologie*. Springer, Berlin/Heidelberg, 275-277.
- Holdermann, S. (1996). *Steinacker. Eine Freilandfundstelle des Mittleren Jungpaläolithikums im Markgräfler Hügelland, Gmde. Müllheim, Ldkr. Breisgau-Hochschwarzwald*. Unpublished Magisterarbeit Tübingen.
- Huntley, D. J. & Lamothe, M. (2001). Ubiquity of anomalous fading in K-feldspars and the measurement and correction for it in optical dating. *Canadian Journal of Earth Sciences* 38: 1093-1106.
- Kadereit, A., Kühn, P. & Wagner, G. (2010). Holocene relief and soil changes in loess-covered areas of south-western Germany: The pedosedimentary archives of Bretten-Bauerbach (Kraichgau). *Quaternary International* 222: 96-119.
- Kaiser, M. J. (2013). *Werkzeug - Feuerzeug - Edelstein. Die Silices des südöstlichen Oberrheingebietes und ihre Nutzung von den Anfängen bis zur Gegenwart*. Materialhefte zur Archäologie in Baden-Württemberg Heft 95, Stuttgart, Theiss Verlag.
- Kasielke, T., Poch, R. M. & Wiedner, K. (2019). Chernozem relics in the Hellweg Loess Belt (Westphalia, NW Germany) - natural or man-made? *Quaternary International* 502: 296-308.
- Kind, C.-J. (2008). Neue Untersuchungen in der Magdalénien-Freilandfundstelle Munzingen, Stadt Freiburg. *Arch. Ausgr. Baden-Württemberg* 2007: 28-32.
- Koehler, H., Griselin, S., Bachelier, F., Bignon-Lau, O. & Mevel, L. (2019). Neue Ergebnisse zum Jüngeren Magdalénien im Elsass. Die Fundstellen Morschwiller-le-Bas und Wolschwiller (Dép. Haut-Rhin, Frankreich). In: H. Floss (Ed.), *Das Magdalénien in Südwestdeutschland, im Elsass und in der Schweiz*, Tübingen.
- Koehler, H., Wegmüller, F., Audiard, B., Auguste, P., Bahain, J.-J., Bocherens, H., Diemer, S., Preusser, F., Pümpin, C., Sévêque, N., Stoetzel, E., Tombret, O. & Wuscher, P. (2021). The Middle Paleolithic Occupations of Mutzig-Rain (Alsace, France). In: H. Koehler, N. J. Conard, H. Floss & A. Lamotte (Eds.), *The Rhine During the Middle Paleolithic: Boundary or Corridor?* Tübingen, Kerns Verlag.
- Krauss, L., Kappenberg, A., Zens, J., Kehl, M., Schulte, P., Zeeden, C., Eckmeier, E. & Lehmkuhl, F. (2018). Reconstruction of late Pleistocene paleoenvironments in southern Germany using two high-resolution loess-paleosol records. *Paleogeography, Paleoclimatology, Paleoecology* 509: 58-76.
- Kreutzer, S., Schmidt, C., Fuchs, M. C., Dietze, M., Fischer, M. & Fuchs, M. (2012). Introducing an R package for luminescence dating analysis. *Ancient TL* 30: 1-8.
- Kreutzer, S., Schmidt, C., DeWitt, R. & Fuchs, M. (2014). The a-value of polymineral fine grain samples measured with the post-IR IRSL protocol. *Radiation Measurements* 69: 18-29.
- Kreutzer, S., Burow, C., Dietze, M., Fuchs, M., Schmidt, C., Fischer, M., Friedrich, J., Mercier, N., Philippe, A., Riedesel, S., Autzen, M., Mittelstrass, D. & Gray, H. (2021). *Luminescence: Comprehensive Luminescence Dating Data Analysis*. R package version 0.9.15, <https://CRAN.R-project.org/package=Luminescence>.
- Kuhn, P., Techmer, A. & Weidenfeller, M. (2013). Lower to middle Weichselian pedogenesis and paleoclimate in Central Europe using combined micromorphology and geochemistry: the loess-paleosol sequence of Alsheim (Mainz Basin, Germany). *Quaternary Science Reviews* 75: 43-58.
- Kühn, P., Lehndorff, E. & Fuchs, M. (2017). Lateglacial to Holocene pedogenesis and formation of colluvial deposits in a loess landscape of Central Europe (Wetterau, Germany). *Catena* 154: 118-135.
- Lais, R. (1929-32). Ein Werkplatz des Azilio-Tardenoisien am Isteiner Klotz. *Badische Fundberichte* 2: 97-115.
- Lass, G. (1994). *Gebrauchsspurenuntersuchungen an den "Mikrolithen" der Sesselfsgrotte*. Münster.
- Lehmkuhl, F., Zens, J., Krauß, L., Schulte, P. & Kels, H. (2016). Loess-paleosol sequences at the northern European loess belt in Germany: distribution, geomorphology and stratigraphy. *Quaternary Science Review*. 153: 11-30.
- Lehmkuhl, F., Nett, J. J., Pötter, S., Schulte, P., Sprafke, T., Jary, Z., Antoine, P., Wacha, L., Wolf, D., Zerboni, A., Hošek, J., Markowicz, S. B., Obrecht, I., Sümehi, P., Veres, D., Zeeden, C., Boemke, B., Schaubert, V., Viehweger, J. & Hambach, U. (2021). Loess landscapes of Europe – Mapping, geomorphology, and zonal differentiation. *Quaternary Science Reviews* 215: 103496.
- Mähling, W. (1978). Eine bemerkenswerte spätpaläolithische Waffenspitze aus dem Markgräflerland. *Archäologische Nachrichten aus Baden* 21: 4-11.
- Mauz, B., Packman, S. & Lang, A. (2006). The alpha effectiveness in silt-sized quartz: new data obtained by single and multiple aliquot protocols. *Ancient TL* 24: 47-52.
- McKeague, J. A., Guertin, R. K., Valentine, K. W. G., Belisle, J., Bourbeau, G. A., Michalyna, W., Hopkins, L., Howell, L., Page, F. & Bresson, L. M. (1980). Variability of estimates of illuvial clay in soils by micromorphology. *Soil Science* 129: 386-388.
- Mieg, M. (1901). Note sur une station de l'époque paléolithique découverte à Istein (Grand-Duché de Bade). *Bulletin de Séances de la Société de Sciences de Nancy* 3/2: 3-6.
- Miller, C. E., Goldberg, P. & Berna, F. (2013). Geoarchaeological investigations at Diepkloof Rock Shelter, Western Cape, South Africa. *Journal of Archaeological Science* 40: 3432-3452.
- Moine, O., Antoine, P., Hatté, C., Landais, A., Mathieu, J., Prud'homme, C. & Rousseau, D. (2017). The impact of Last Glacial climate variability in west-European loess revealed by radiocarbon dating of fossil earthworm granules. *PNAS* 114: 6209-6214.
- Moreau, L. (2009). *Geißenklösterle - Das Gravettien der Schwäbischen Alb im europäischen Kontext*. Tübingen, Kern Verlag.
- Moreau, L. (2014). A newly discovered shaft smoother from the open air site Steinacker, Breisgau-Hochschwarzwald district (Baden-Württemberg, Germany). *Quartär* 61: 159-164.
- Nicosia, C. & Stoops, G. (2017). *Archaeological Soil and Sediment Micromorphology*. Oxford.
- Padtberg, A. (1925). *Das altsteinzeitliche Lößlager bei Munzingen nach eigenen Ausgrabungen*. Augsburg, Filser.
- Pasda, C. (1994). *Das Magdalénien in der Freiburger Bucht*. Materialh. Arch. Baden-Württemberg 25, Stuttgart, Theiss.
- Pasda, C. (1998a). Der Beginn des Magdalénien in Mitteleuropa. *Archäologisches Korrespondenzblatt*. 28: 175-190.
- Pasda, C. (1998b). *Wildbeuter im archäologischen Kontext – Das Paläolithikum in Südbaden*. Folio-Verlag Wesselkamp, Bad Bellingen.
- Pasda, C. (2000). Zur Verwendung von Silexrohstoffen in der Steinzeit Südbadens. *Archäologische Nachrichten aus Baden* 62: 7-15.
- Pasda, C. (2017). Munzingen - A Magdalénien site in the southern Upper Rhine Plain (Germany). In: C. Bourdier et al. (Eds.), *L'essor du Magdalénien. Aspects culturels, symboliques et techniques des faciès à Navettes et à Lussac-Angles*. Séanc. Soc. Préhist. Française 8, Paris, 157-173.
- Pasda, C. (2019a). Das Magdalénien an Hoch- und Oberrhein in Baden und der Pfalz. In: H. Floss (Ed.), *Das Magdalénien in Südwestdeutschland, im Elsass und in der Schweiz*, Tübingen, 131-158.

- Pasda, C. (2019b).** Versuch einer zeitlichen Gliederung des Magdaléniens in Südwest-deutschland. In: M. Baales & C. Pasda (Eds.), „All der holden Hügel ist keiner mir fremd...“ – Festschr. C.-J. Kind. Univ. Forsch. Prähist. Arch. 327, Bonn, Habelt, 259-278.
- Peters, E. (1930).** *Die altsteinzeitliche Kulturstätte Petersfels.* Augsburg.
- Pfeifer, S.J. (2016).** *Die Geweihfunde der magdalénienzeitlichen Station Petersfels, Lkr. Konstanz – eine archäologisch-taphonomische Studie.* Forschungen und Berichte zur Archäologie in Baden-Württemberg 3. Wiesbaden, L. Reichert.
- R Core Team (2021).** *R: A language and environment for statistical computing.* R Foundation for Statistical Computing, Vienna, Austria. URL <https://www.R-project.org/>.
- Roberts, H.M. & Wintle, A.G. (2001).** Equivalent dose determinations for polymineralic fine-grains using the SAR protocol: application to a Holocene sequence of the Chinese Loess Plateau. *Quaternary Science Reviews* 20: 859-863.
- Sainty, J. & Thévenin, A. (1978).** Le sol 74. *Rech. Geogr. Strasbourg* 7: 123-137
- Sauer, D., Kadereit, A., Kühn, P., Kösel, M., Miller, C.E., Shinonaga, T., Kreutzer, S., Herrmann, L., Fleck, W., Starkovich, B.M. & Stahr, K. (2016).** The loess-paleosol sequence of Datthausen, SW Germany: characteristics, chronology, and implications for the use of the Lohne soil as a marker soil. *Catena* 146: 10–29.
- Schmidt, C., Böskén, J. & Kolb, T. (2018).** Is there a common alpha-efficiency in polymineral samples measured by various infrared stimulated luminescence protocols? *Geochronometria* 45: 160-172.
- Schoetensack, O. (1908).** *Der Unterkiefer des Homo Heidelbergensis aus den Sanden von Mauer bei Heidelberg. Ein Beitrag zur Paläontologie des Menschen.* Leipzig.
- Schumacher, E. (1897).** Über das erste Auftreten der Menschen im Elsass. *Mitt. Philom. Ges. Elsaß-Lothringen* 1: 93-117.
- Solich, M. & Bradtmöller, M. (2017).** Socioeconomic complexity and the resilience of hunter-gatherer societies. *Quaternary International* 446: 109-127.
- Stoops, G. (2003).** *Guidelines for analysis and description of soil and regolith thin sections.* Soil Science Society of America, Madison.
- Taller, A. & Conard, N. (2019).** Transition or replacement? Radiocarbon dates from Hohle Fels cave (Alb-Donau-Kreis/D) and the passage from Aurignacian to Gravettian. *Archäologisches Korrespondenzblatt* 49: 165-181.
- Thévenin, A. & Sainty, J. (1980).** Une gisement préhistorique exceptionnel du Jura al-sacien: l'abri du Mannlefelsen I à Oberlarg (Haut-Rhin). *Annuaire de la Société d'Histoire Sundgauvienne*: 21-39.
- Trandafir, O., Timar-Gabor, A., Schmidt, C., Veres, D., Anghelinu, M., Hambach, U. & Simon, S. (2015).** OSL dating of fine and coarse quartz from a Paleolithic sequence on the Bistrița Valley (Northeastern Romania). *Quaternary Geochronology* 30: 487-492.
- Uthmeier, T. (2004).** *Micoquien, Aurignacien und Gravettien in Bayern: Eine regionale Studie zum Übergang vom Mittel- zum Jungpaläolithikum.* Archäologische Berichte 18. Heidelberg: Propylaeum.
- Wintle, A. G. & Murray, A. S. (2006).** A review of quartz optically stimulated luminescence characteristics and their relevance in single-aliquot regeneration dating protocols. *Radiation Measurements* 41: 369-391.
- van Huissteden, K. & Pollard, D. (2003).** Oxygen isotope stage 3 fluvial and eolian successions in Europe compared with climate model results. *Quaternary Research* 59: 223–233.
- Zotz, L. F. (1928).** Die paläolithische Besiedlung der Teufelsküchen am Ölberg beim Kuckucksbad. *Prähistorische Zeitschrift* 19: 3-53.

Inhalt - Contents

Spatial use at Große Grotte (Blaubeuren, Southern Germany), and Implications for Middle Paleolithic Stratigraphy, Spatiality and Chronology

Raumnutzung in der Großen Grotte (Blaubeuren, Süddeutschland) und Implikationen für die mittelpaläolithische Stratigraphie, Räumlichkeit und Chronologie

Jens Axel FRICK, Benjamin SCHÜRCH & Berrin ÇEP.....7-27

Exploring a novelty in the Middle Palaeolithic of Croatia: Preliminary data on the open-air site of Campanož

Erste Daten zu der neu entdeckten mittelpaläolithischen Freilandfundstelle Campanož in Kroatien

Marko BANDA, Francesca ROMAGNOLI, Darko KOMŠO, Maja ČUKA & Ivor KARAVANIĆ.....29-56

Living on the slope. The Middle and Upper Paleolithic occupation of Feldberg "Steinacker"

Leben auf dem Hang. Die mittel- und jungpaläolithische Besiedlung von Feldberg "Steinacker"

Marcel BRADTMÖLLER, Olaf BUBENZER, Stefan HECHT, Diethard TSCHOCKE, Aitor CALVO, Arantzazu Jindriska PÉREZ FERNÁNDEZ, Christoph SCHMIDT, Joao MARREIROS,

Felix HENSELOWSKY, Merlin HATTERMANN, Lisa BAUER & Marcel EL-KASSEM.....57-84

Technological and functional analysis of Upper Palaeolithic backed micro-blades from southern Oman

Technologische und funktionale Analyse jungpaläolithischer Mikroklingen aus dem südlichen Oman

Yamandú H. HILBERT, Ignacio CLEMENTE-CONTE, Matthias LÓPEZ CORREA, Najat AL-FUDHAILI & Claudio MAZZOLI.....85-103

Investigations at the Epigravettian site of Barmaky in Volhynia, north-west Ukraine: analyses and taxonomic reflections

Untersuchungen am Epigravettien-Fundplatz Barmaky in Volhynia, Nordwest-Ukraine: Analysen und taxonomische Überlegungen

Victor CHABAI, Diana DUDNYK, Kerstin PASDA, Michael BRANDL & Andreas MAIER.....105-144

Grooves on the cortex of the Epigravettian lithic industry in the broader context

Rillen auf der Kortex von Steinartefakten des Epigravettien im weiteren Kontext

Zdeňka NERUDOVA & Petr LEPCIO.....145-161

Rivers run and people may meander. Water body-oriented land use decisions in the Neuwied Basin during the Late Upper Palaeolithic and Late Palaeolithic

Fluss im Lauf und Lauf am Fluss. Wasser-orientierte Landnutzungsentscheidungen im Neuwieder Becken während des späten Jungpaläolithikums und Spätpaläolithikums

Tjaark SIEMSEN & Andreas MAIER.....163-177

A caribou hunting drive at Nernartuut (Nuussuaq, Northwest Greenland)

Eine Karibu-Jagdanlage bei Nernartuut (Nuussuaq, Nordwestgrönland)

ClemensPASDA.....179-202

Book review

Buchbesprechung.....203-205